CHAPTER V

SEDIMENTARY PETROGRAPHY OF THE LANDFORMS

In this chapter the following sedimentary petrography properties of particular landforms will be discussed including roundness of pebbles, pebble association, and also grain size of the particles < 2000 μ.

Samples from fieldwork were manually prepared for laboratory analysis based on their stratigraphic integrity in order to classify any kinds and characteristics of such a sediment. The analysis of sediment from each particular landform leads to the understanding of depositional process as well as much more accuracy of the final interpretation of the environment of deposition.

Gravels using for morphometrical gravel and pebble composition analyses were collected totally 53 samples mostly from terrace surface and terrace profiles. Fifty sampling gravels within one square-meter are designed and collected consequently in each location. 72 samples using for grain size analysis were collected, which represented individually of each specific landform unit. Locations of gravels sampling and grain size analysis sampling are shown in Figure 5.1. The result of each samples will finally be explained and then illustrated in forms of histograms, 100% stack column, and graphs.

Pebble roundness

The roundness of pebbles was measured according to the method described in Chapter II. In Figure 5.2 the result are represented graphically by frequency histograms. The horizontal axis represents roundness index intervals, which are plotted in range of 100, whereas, the vertical axis shows the percentages of pebbles with roundness indices within such a range.

Frequency histograms of roundness indices of gravels are presented together with the histograms of flatness-indices. The roundness indices of river gravels from the study area show maximum values in the subrounded and rounded, well-rounded class (100-200, 200-300, and >300 respectively). The occurrence of pebbles up to 500 class indicates that in general the pebbles are rounded to well-rounded. The high degree of

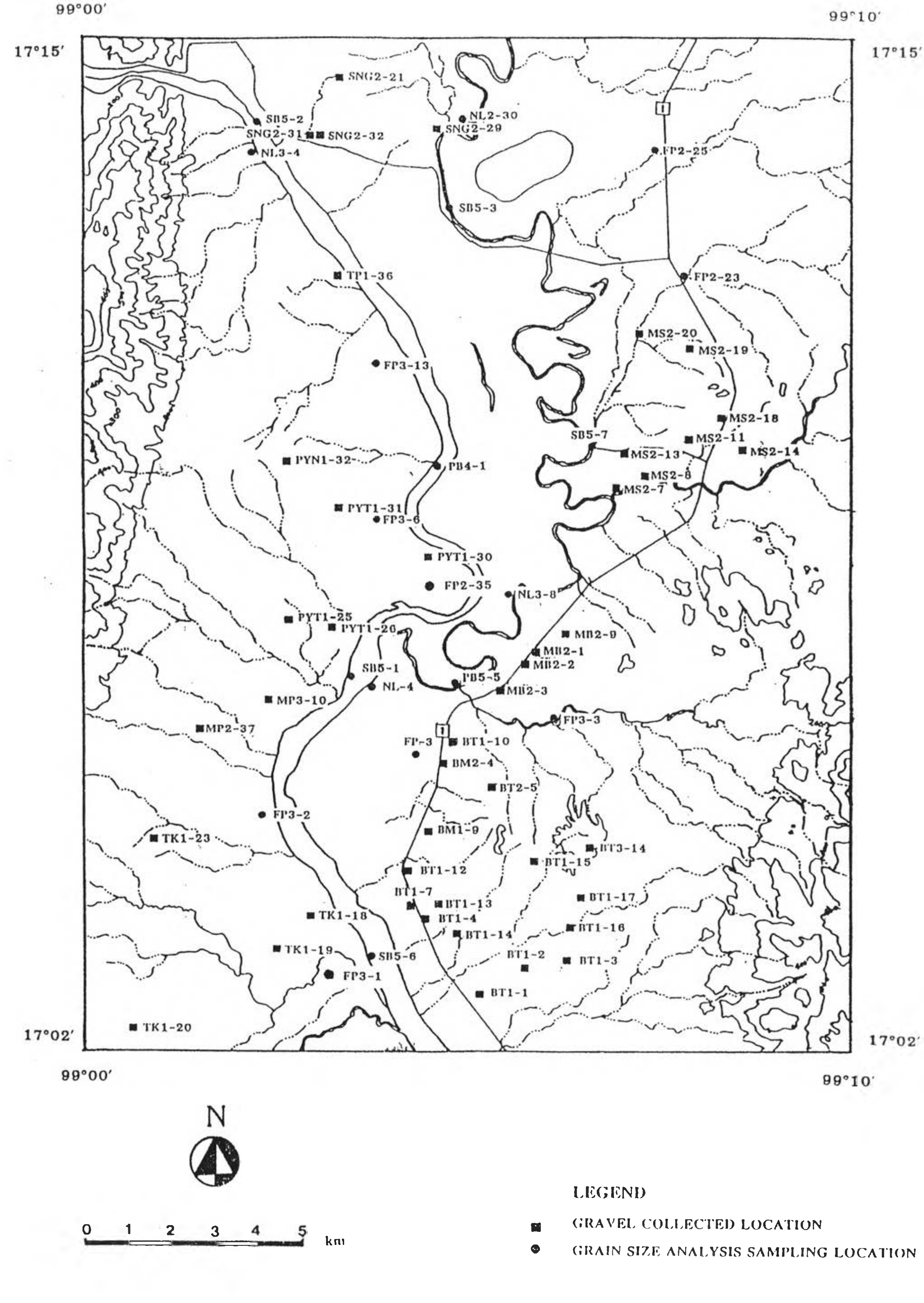

Figure 5.1 Location of gravels sampling and grain size analysis sampling position.

smoothness of the gravels confirms their deposition by some kind of fluvial process and most likely by rivers (Thiramongkol, 1975). An alternative origin, that of marine deposition can probably by excluded because of the low flatness values of the pebbles (Thiramongkol, 1975). Thus, the degree of flatness will not be explained in this part.

Figures 5.2-5.6 represent the roundness indices of pebbles with a maximal diameter < 4 cm of Tertiary landform unit, whereas those of high terrace, middle, and low terraces are shown in Figures 5.7-5.10, 5.11-5.12, and 5.13, respectively. All morphometrical gravel analyses of stones are summarized below and illustrated by histograms as follows.

In Tertiary landform unit, 24 gravel samples were collected mostly within restricted ground and gravel bed of road cut and stream cut profile. The roundness of pebbles of Ban Tak and Mae Bon terrace parts is represented graphically in Figures 5.2-5.6.

Gravels from Ban Tak Tertiary landform unit contains 19 samples, which collected from different sites. The roundness of all samples ranges from rounded to well-rounded, excepting samples no. BT1-7D, BT1-7E, and BT2-4, which show difference in subrounded indices.

Samples no. BT1-7D, BT1-7E, and BT1-4 of Ban Tak Tertiary landform unit represented subrounded indicating quite a short distance of transportation, which reasonably equivalent with their lithology. As will be shown in next result, gravels of samples no. BT1-7D, BT1-7E, and BT2-4 are composed abundantly of subrounded schist.

5 samples from Mae Bon Tertiary landform unit are represented in Figure 5.6 with the percentage of indices > 200. The roundness of all samples is ranging from rounded to well-rounded.

Samples of high terrace are represented in Figures 5.7 to 5.10 including 9 samples from Sam Ngao high terrace (Figure 5.7), 1 sample from Pa Yang Nua high terrace and 1 sample from Tha Pui high terrace (Figure 5.8), and 9 samples from Mae Salid high terrace (Figures 5.9-5.10). The roundness of entire samples is ranging from rounded to well-rounded.

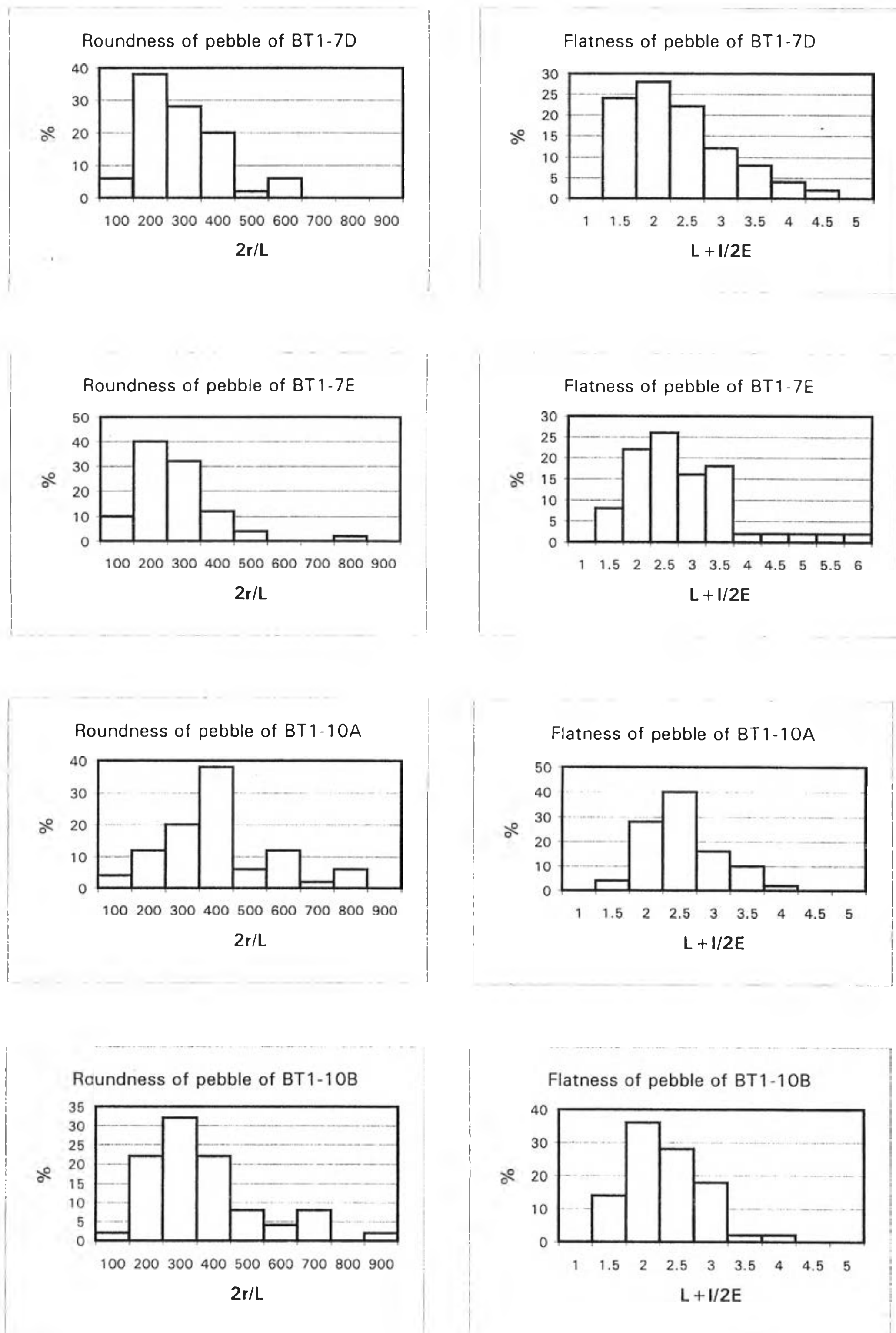

Figure 5.2 The roundness index of samples from Ban Tak Tertiary landform unit.

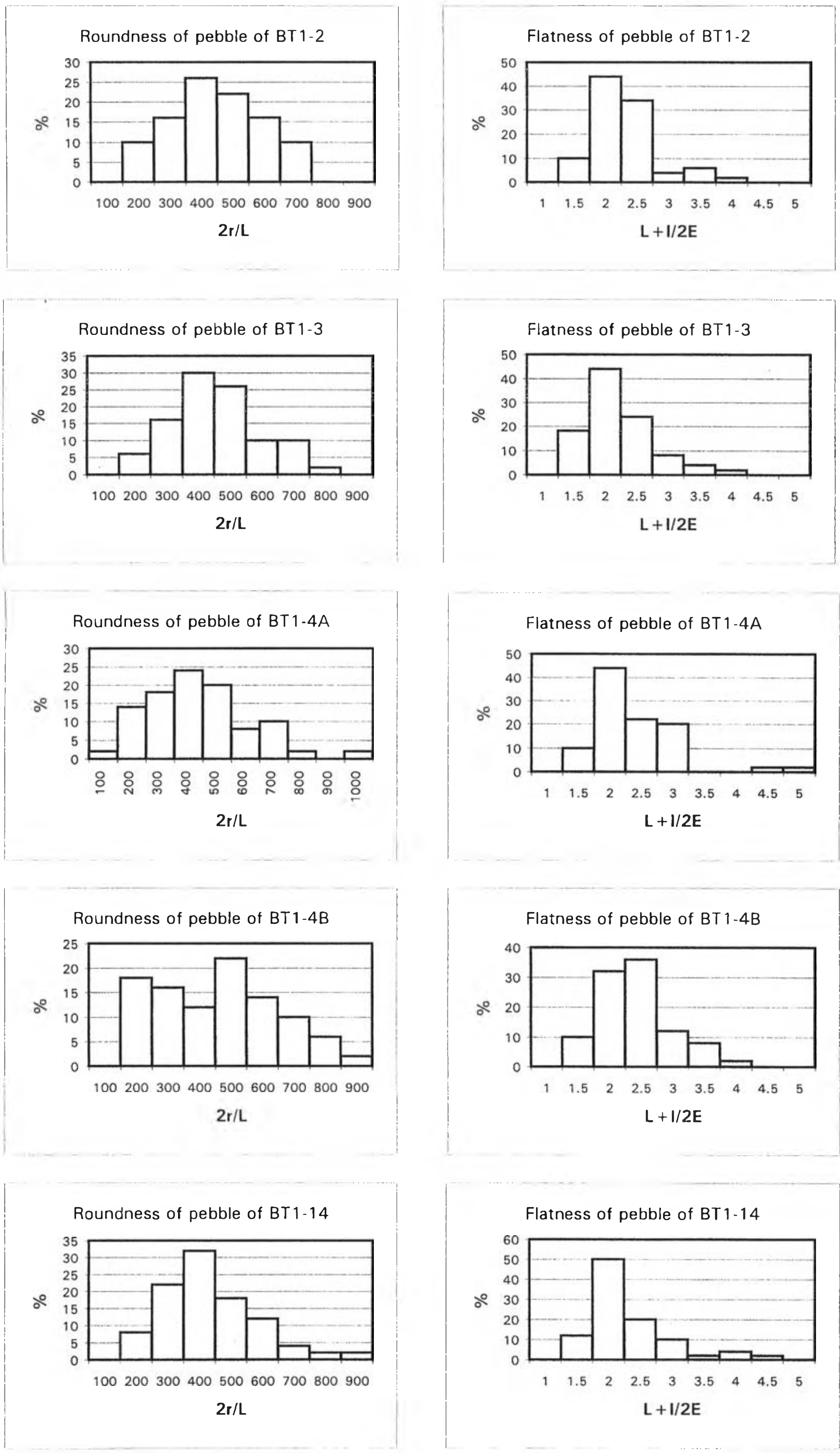

Figure 5.3 The roundness index of samples from Ban Tak Tertiary landform unit.(cont.)

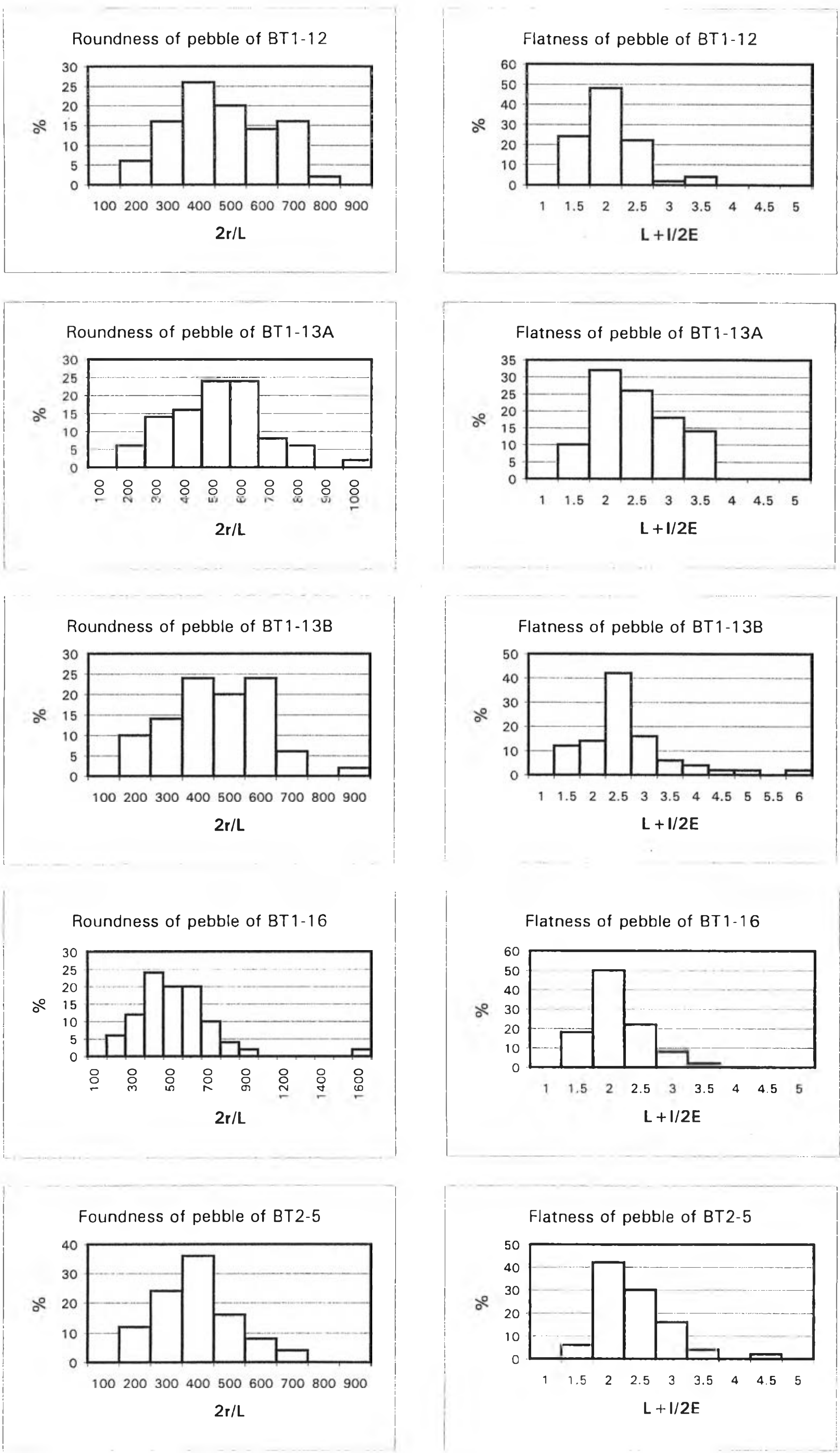

Figure 5.4 The roundness index of samples from Ban Tak Tertiary landform unit.(cont.)

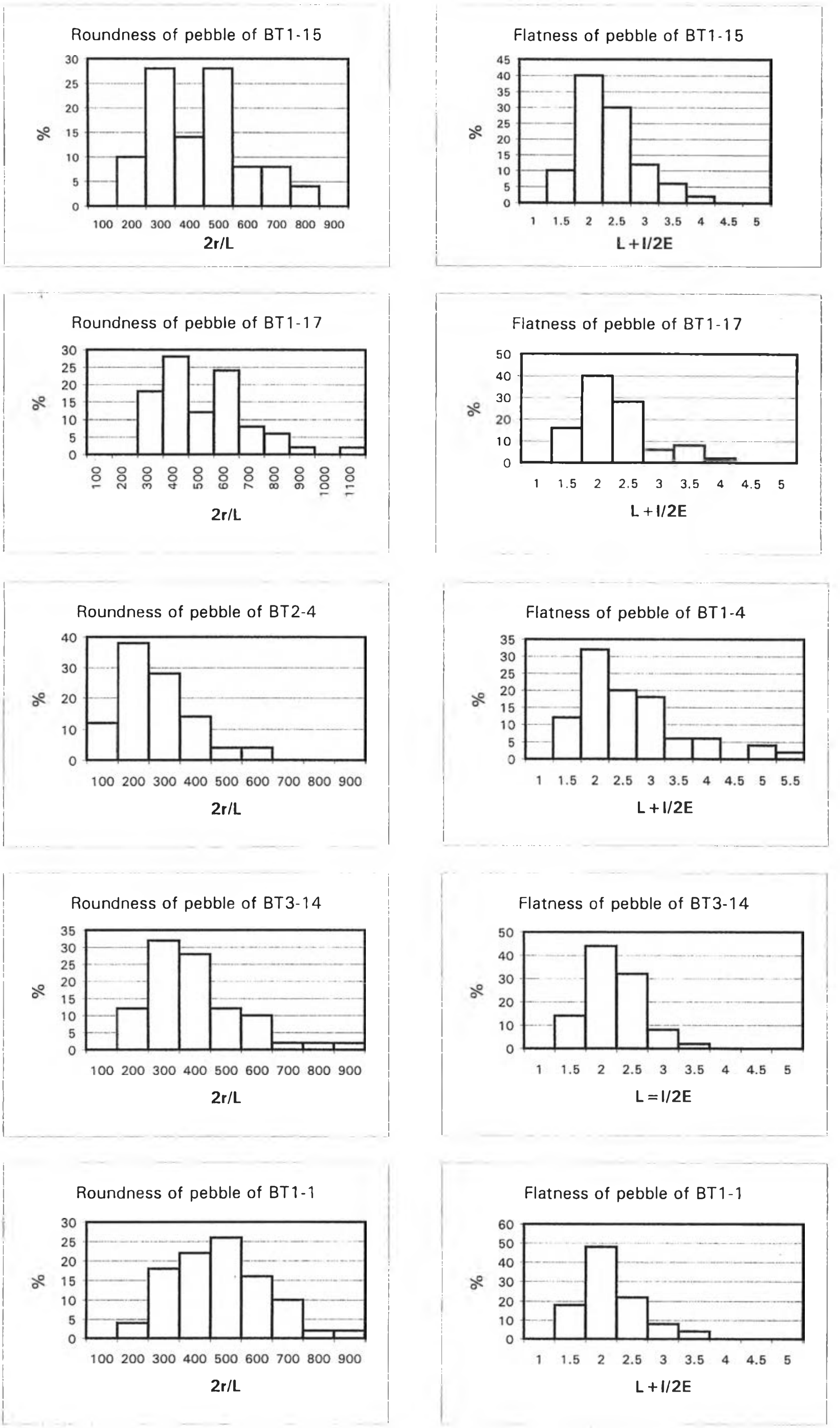

Figure 5.5 The roundness index of samples from Ban Tak Tertiary landform unit.(cont.)

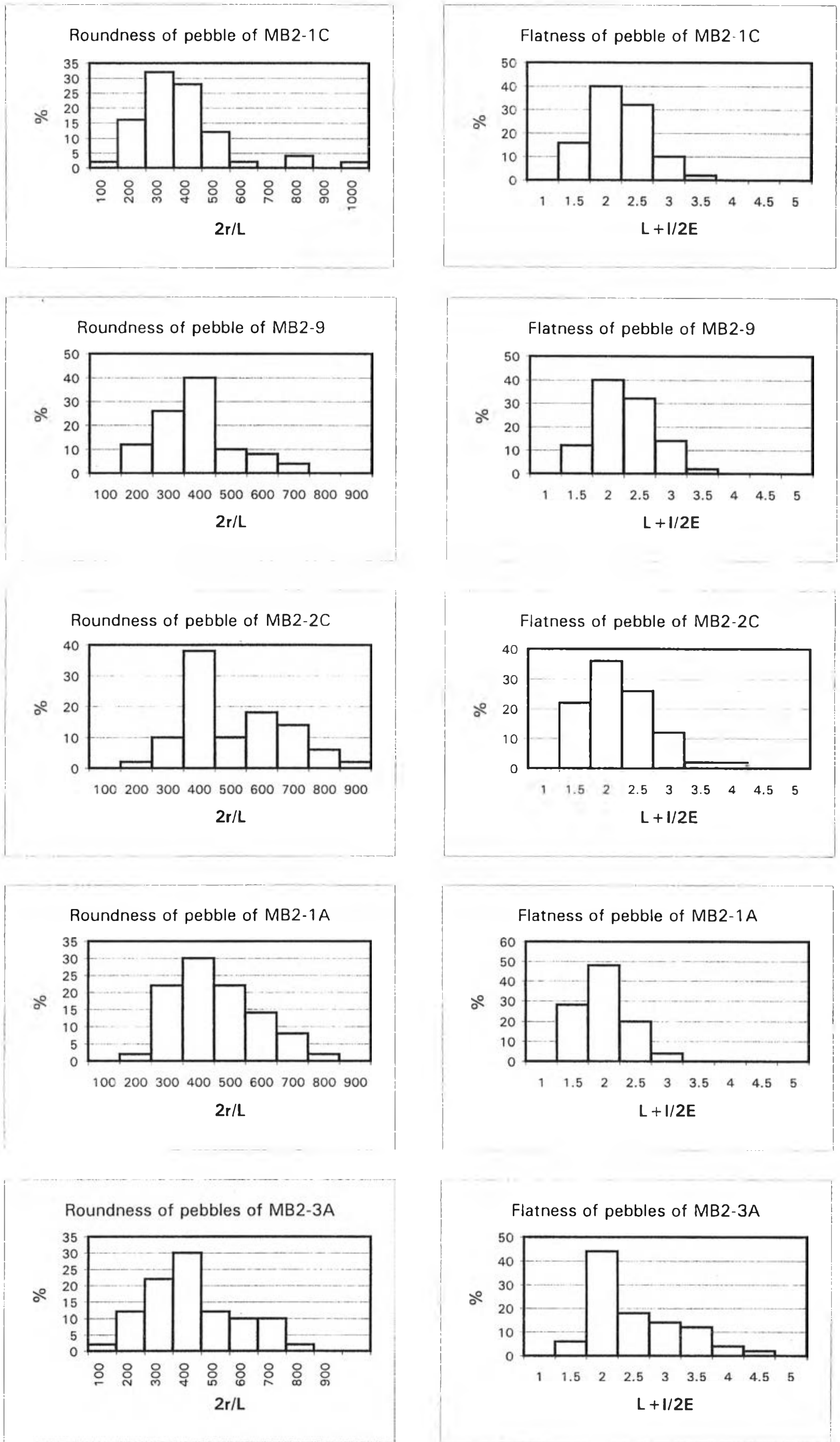

Figure 5.6 The roundness index of samples from Mae Bon Tertiary landform unit.

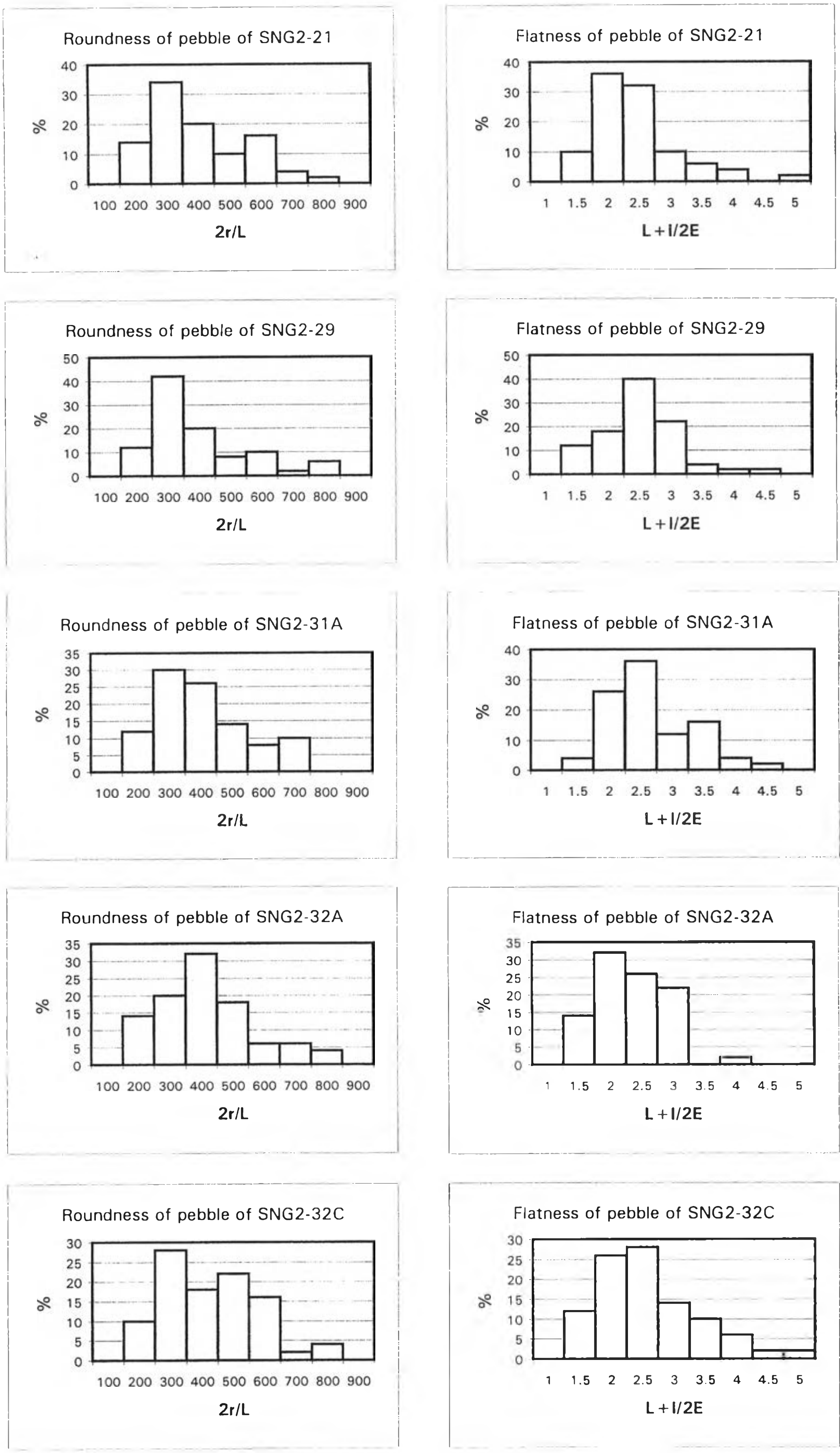

Figure 5.7 The roundness index of samples from Sam Ngao high terrace.

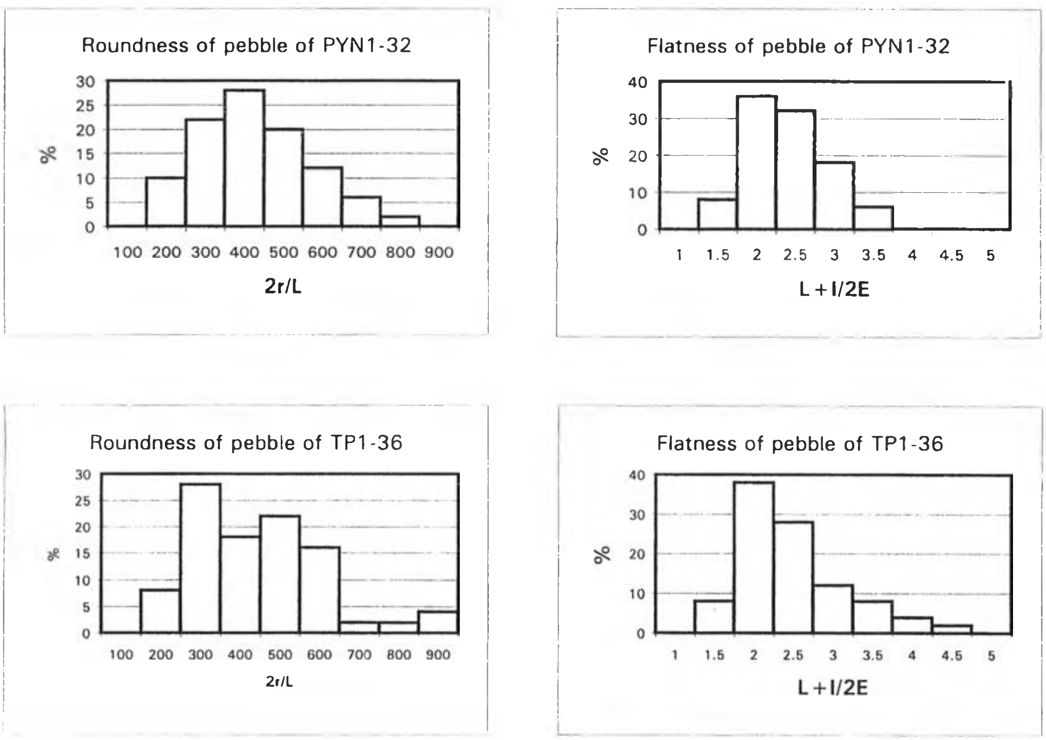

Figure 5.8 The roundness index of samples from Payang Nua high terrace (PYN1-32) and Tha Pui high terrace (TP1-36)

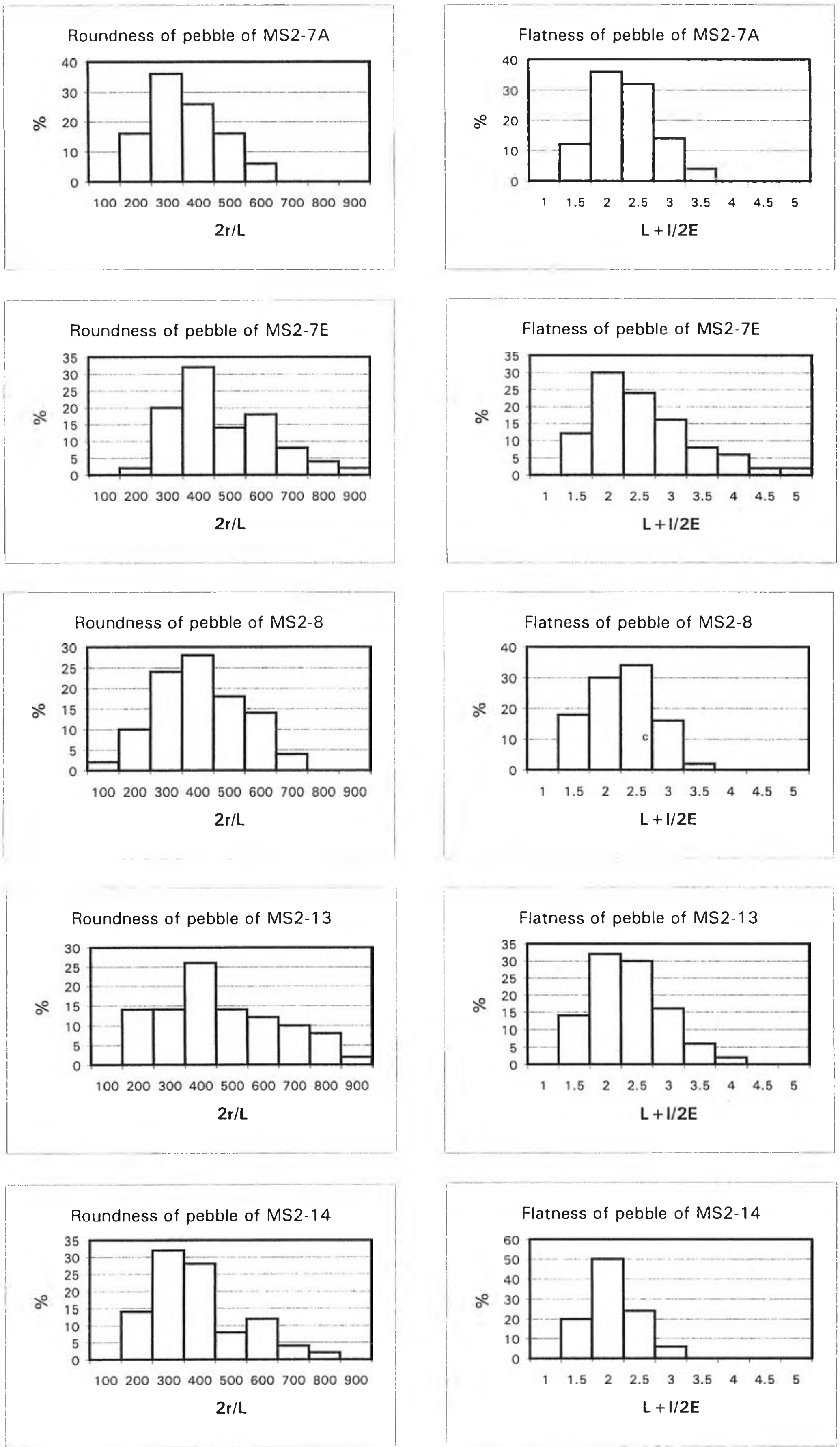

Figure 5.9 The roundness index of samples from Mae Salid high terrace

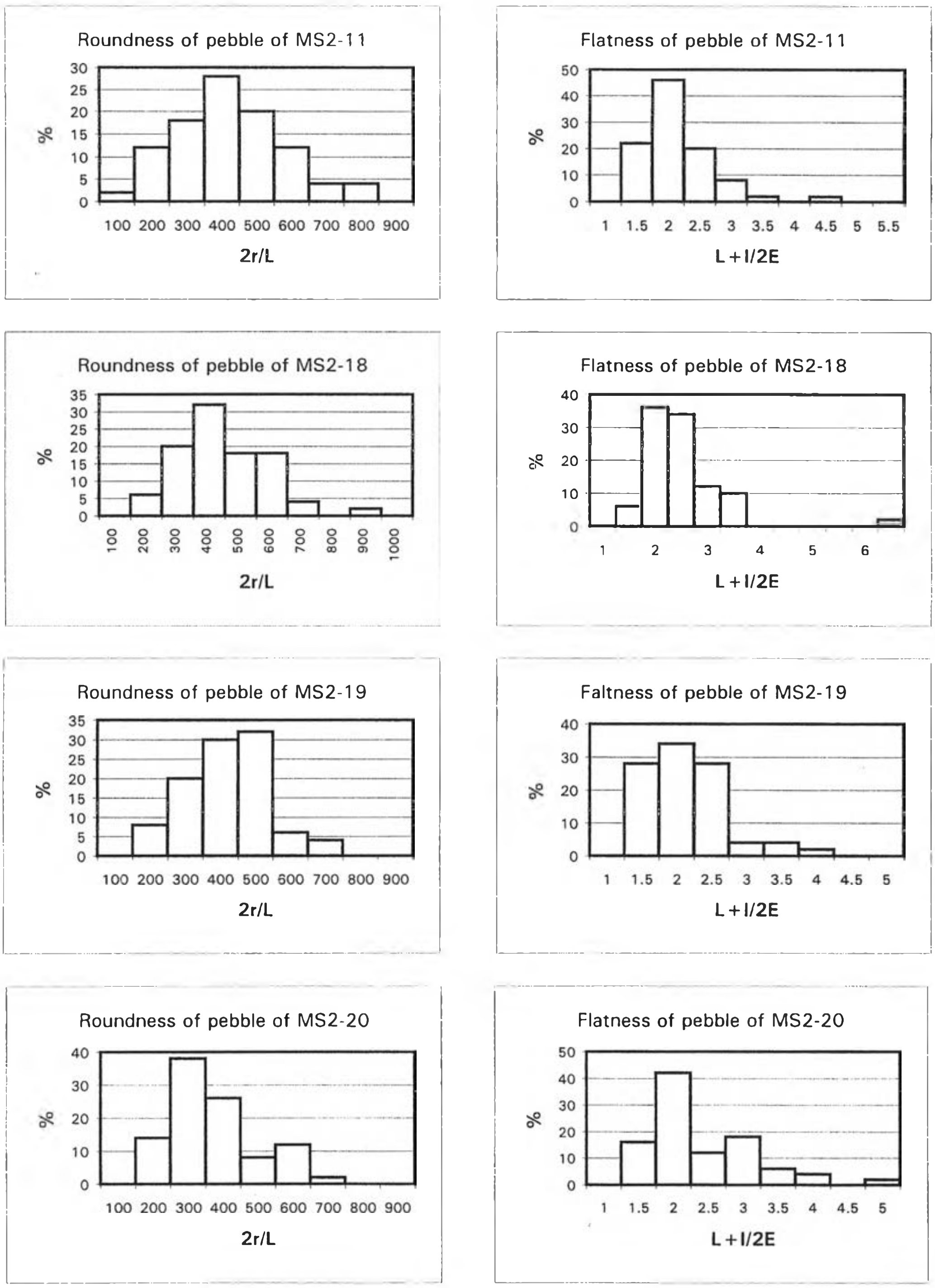

Figure 5.10 The roundness index of samples from Mae Salid high terrace. (cont.)

Samples in Figures 5.11 and 5.12 were particularly collected from middle terrace. Figure 5.11 shows roundness indices of samples that collected from Pa Yang Tai middle terrace and Figure 5.12 shows roundness indices of samples that collected from That Khunram middle terrace. The roundness shows subrounded to well-rounded. Partly in some middle terrace, sample no. TK1-18B for example of That Khunram middle terrace, the roundness shows subrounded which is caused by short distance of transportation than the other samples. But in this case, its lithology is also counterpart. As will be shown in the next result, large amount of schist of sample no. TK1-18B causes it shows subrounded indices.

Figure 5.13 shows the roundness of samples from low terrace. Samples no. BM1-9 and BM2-4 were collected from Ban Mai low terrace and samples no. MP3-10 and MP2-37 were kept from Mae Phayuap low terrace. The roundness is well-rounded in samples no. BM1-9, BM2-4, and MP3-10 while sample no MP2-37 shows rounded indices.

Range of roundness of stones calculated by Cailleux method in the study area is summarized as Table 5.1. In conclusion, the average roundness of fluvial stones within the study area is mostly rounded to well-rounded, which indicates long distance of transportation from the sources. The sediments have been transported by fluvial process.

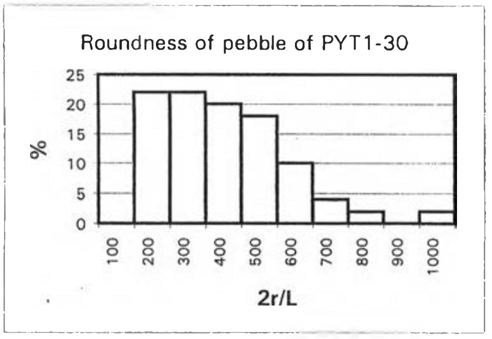

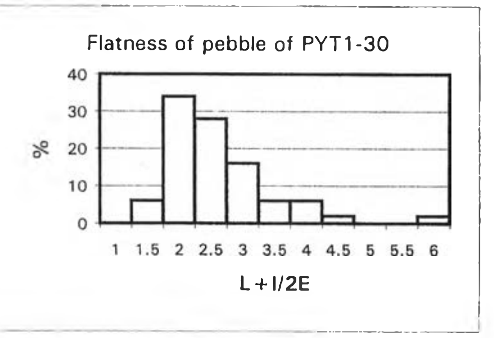

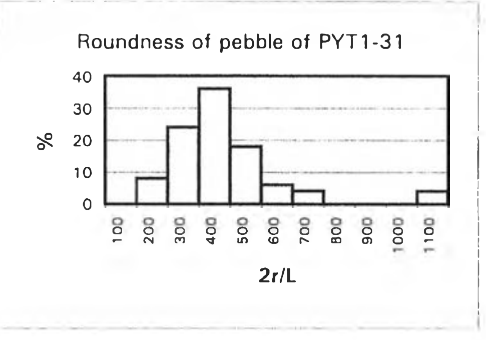

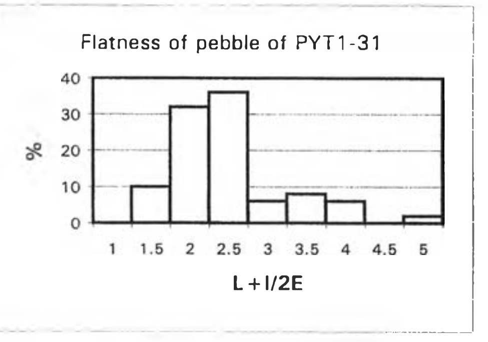

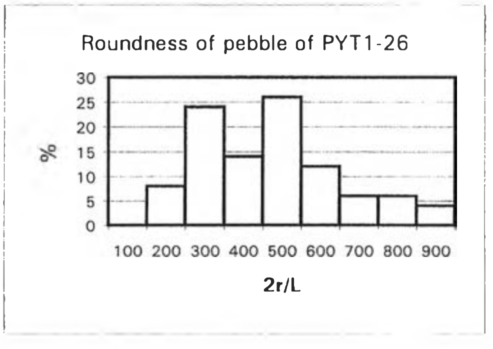

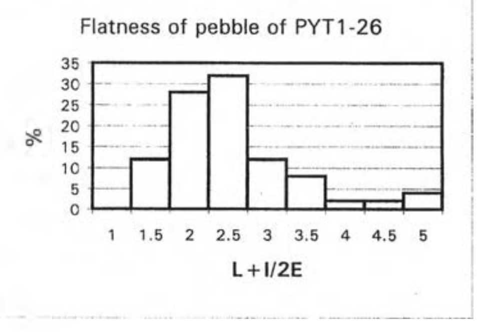

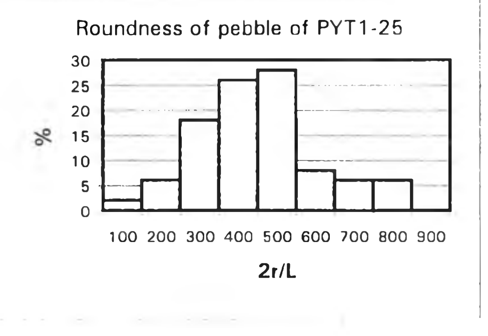

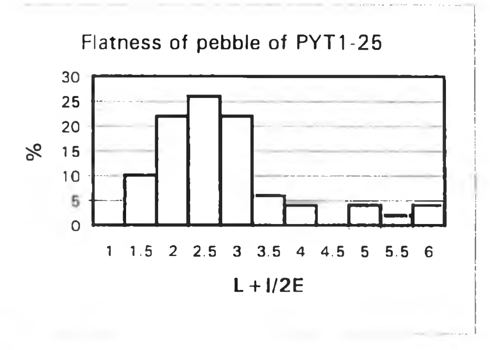

Figure 5.11 The roundness index of samples from Pa Yang Tai middle terrace.

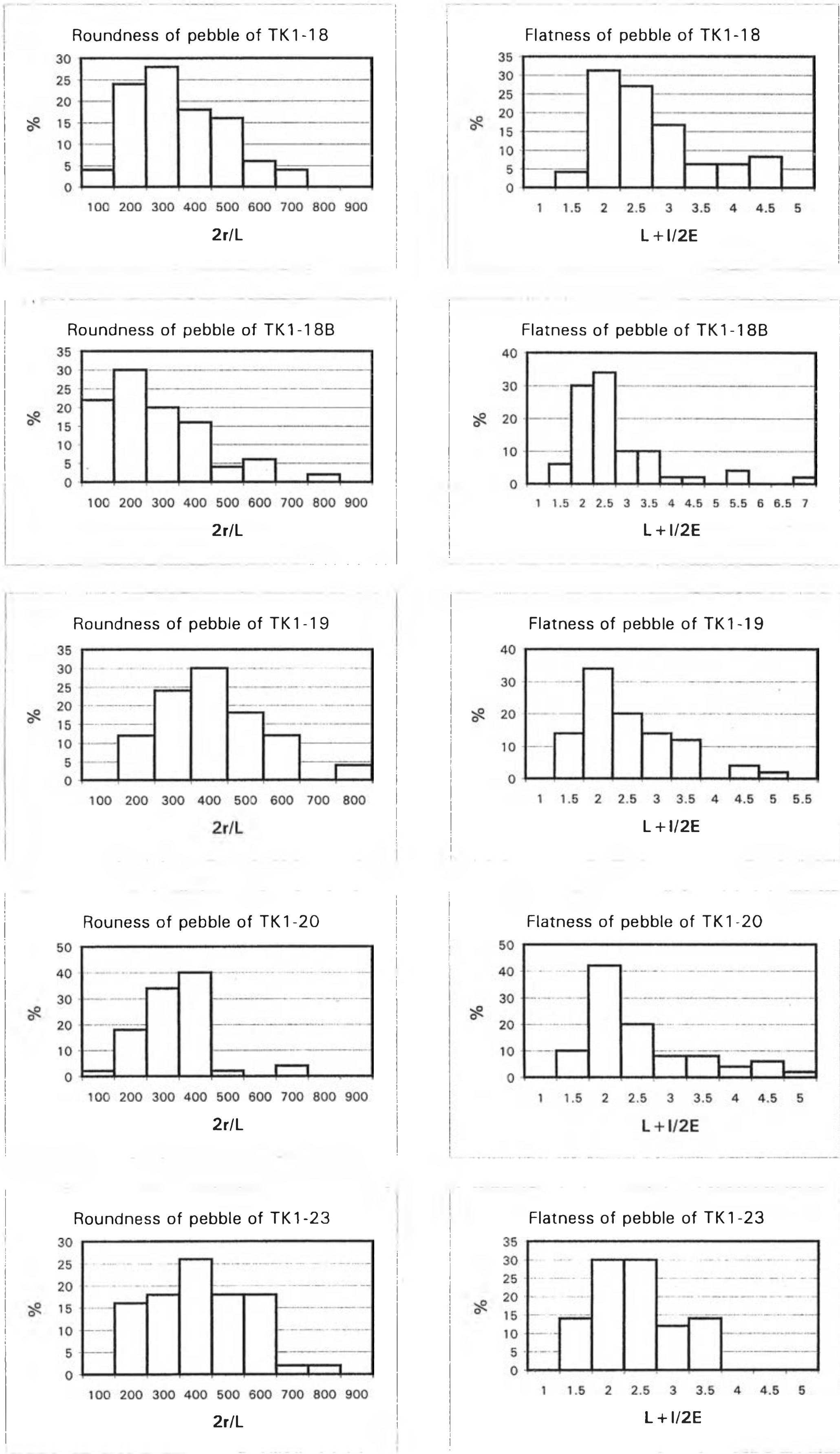

Figure 5.12 The roundness index of samples from That Khunram middle terrace.

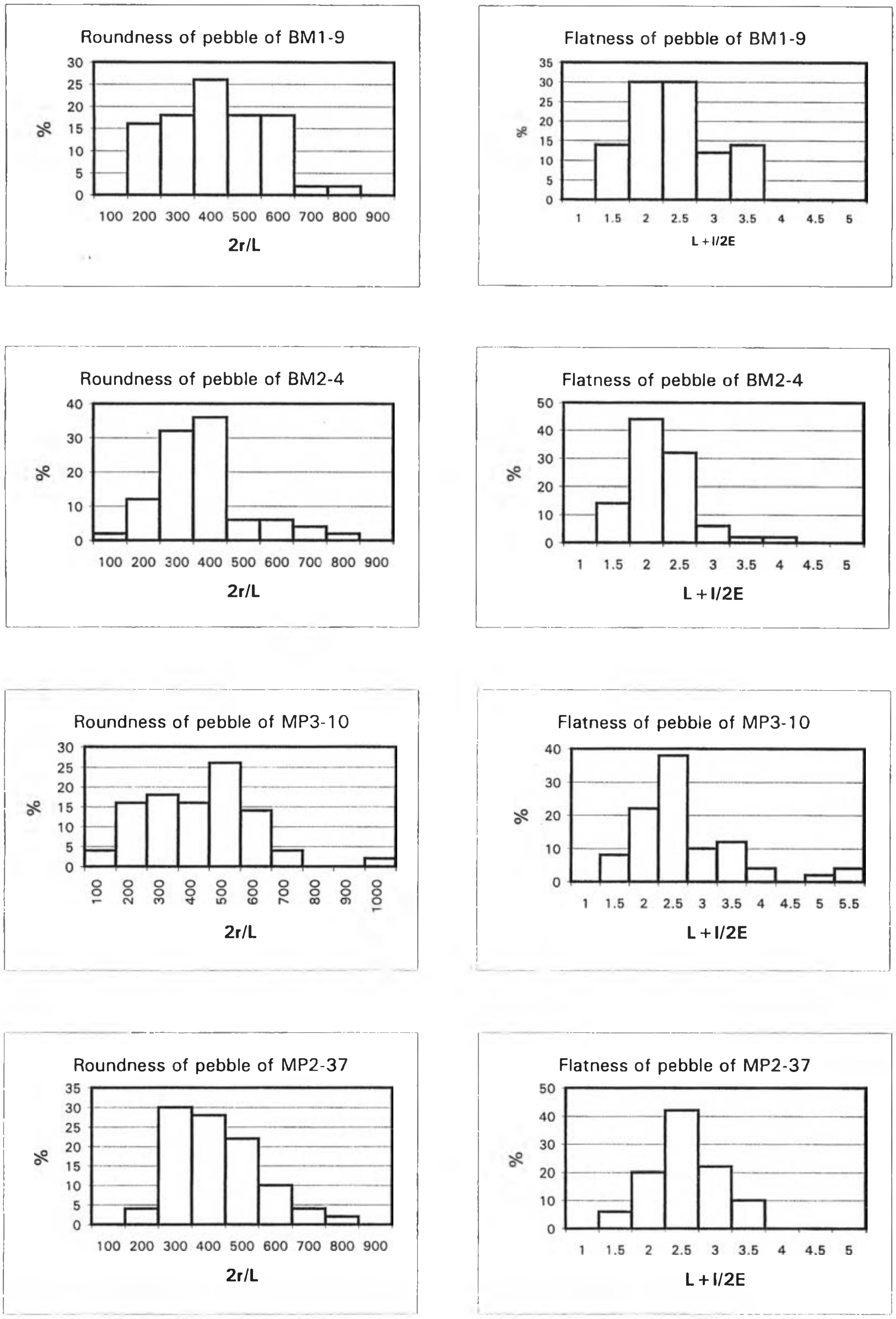

Figure 5.13 The roundness index of samples from Ban Mai low terrace (BM1-9 and BM2-4) and Mae Payuap low terrace (MP3-10 and MP2-37).

Table 5.1 Range of roundness of stones calculated by Cailleux method in the study area.

Sample	A	SA	SR	R	WR	Location	Remark
BT1-1					■	BT	TLU
BT1-2					■	BT	TLU
BT1-3					■	BT	TLU
BT1-4A					■	BT	TLU
BT1-4B					■	BT	TLU
BT1-7D			■			BT	TLU
BT1-7E			■			BT	TLU
BT1-10A					■	BT	TLU
BT1-10B				■		BT	TLU
BT1-12					■	BT	TLU
BT1-13A					■	BT	TLU
BT1-13B					■	BT	TLU
BT1-14					■	BT	TLU
BT1-15				■		BT	TLU
BT1-16					■	BT	TLU
BT1-17					■	BT	TLU
BT2-4			■			BT	TLU
BT2-5					■	BT	TLU
BT3-14				■		BT	TLU
MB2-1A					■	MB	TLU
MB2-1C				■		MB	TLU
MB2-2C					■	MB	TLU
MB2-3A					■	MB	TLU
MB2-9					■	MB	TLU
SNG2-21				■		SNG	HT
SNG2-29				■		SNG	HT
SNG2-31A				■		SNG	HT
SNG2-32A					■	SNG	HT
SNG2-32C				■		SNG	HT
TP1-36					■	TP	HT
PYN1-32				■		PYN	HT

Sample	A	SA	SR	R	WR	Location	Remark
MS2-7A				■		MS	HT
MS2-7E					■	MS	HT
MS2-8					■	MS	HT
MS2-13					■	MS	HT
MS2-14				■		MS	HT
MS2-11					■	MS	HT
MS2-18					■	MS	HT
MS2-19					■	MS	HT
MS2-20				■		MS	HT
PYT1-25					■	PYT	MT
PYT1-26					■	PYT	MT
PYT1-30			■	■		PYT	MT
PYT1-31					■	PYT	MT
TK1-18				■		TK	MT
TK1-18B			■			TK	MT
TK1-19					■	TK	MT
TK1-20					■	TK	MT
TK1-23					■	TK	MT
BM1-9					■	BM	LT
BM2-4					■	BM	LT
MP3-10					■	MP	LT
MP2-37				■		MP	LT

Roundness Class A=Angular

SA=Subangular

SR=Subrounded

R=Rounded

WR=Well rounded

Remark TLU=Tertiary landform unit

HT=High terrace

MT=Middle terrace

LT=Low terrace

Pebble associations

The pebble composition analysis was carried out according to the method described in Chapter II. The results are represented graphically by 100% stack column. It compares the percentage of each value contributing to the total across categories.

Regarding Figure 5.14, some of the most characteristic gravel associations are represented in form of simplified diagram. It designed to represent the gravel composition of the Tertiary landform unit. The percentages of quartzite are plotted from the bottommost, and then up to quartz and those of sandstones and finally, if present, those of metasandstones in the upper. The rest group remains at the uppermost.

In Figures 5.14 and 5.15, gravels of Tertiary landform unit are composed commonly of quartzite, quartz, sandstone and metasandstone. These compositions are expected to have supplied from upstream especially Silurian-Devonian quartzite. However, there are locally schist, pebbly sandstone and breccia. Especially at the lower part of Ban Tak Tertiary landform unit (samples no. BT1-7D, BT1-7E, BT1-10A and BT2-4), the content of schist is up to 40%.

In Figure 5.16, samples from Mae Bon Tertiary landform unit (samples no. MB2-1C and MB2-2C) contain schist about 20% in the lower part of the deposits. The high schist content in the lower part of this unit can be ascribed to have come from upstream Silurian-Devonian schist. However, schist is absent in the other samples.

Figures 5.17 and 5.18 represent the pebble composition of the high terrace group. At Sam Ngao (samples no. SNG2-21, SNG2-29, and SNG2-32A), Tha Pui (TP1-36) and Pa Yang Nua (PYN1-32) high terrace, the gravel consists mostly of quartzite, quartz, sandstone and metasandstone. The content of quartz is ranging from 30-50 % and quartzite is about 10-20 %. Especially, at Pa Yang Nua high terrace, quartz content is up to 80 %. These are supplied by upstream Silurian-Devonian quartzite and also quartz dike. However, samples no. SNG2-32A and C of Sam Ngao high terrace show small amount of schist and granite (<5%).

The pebble composition of Mae Salid high terrace is shown in Figure 5.18. Pebbles in this terrace consist of various components. Whereas the major component of other terrace

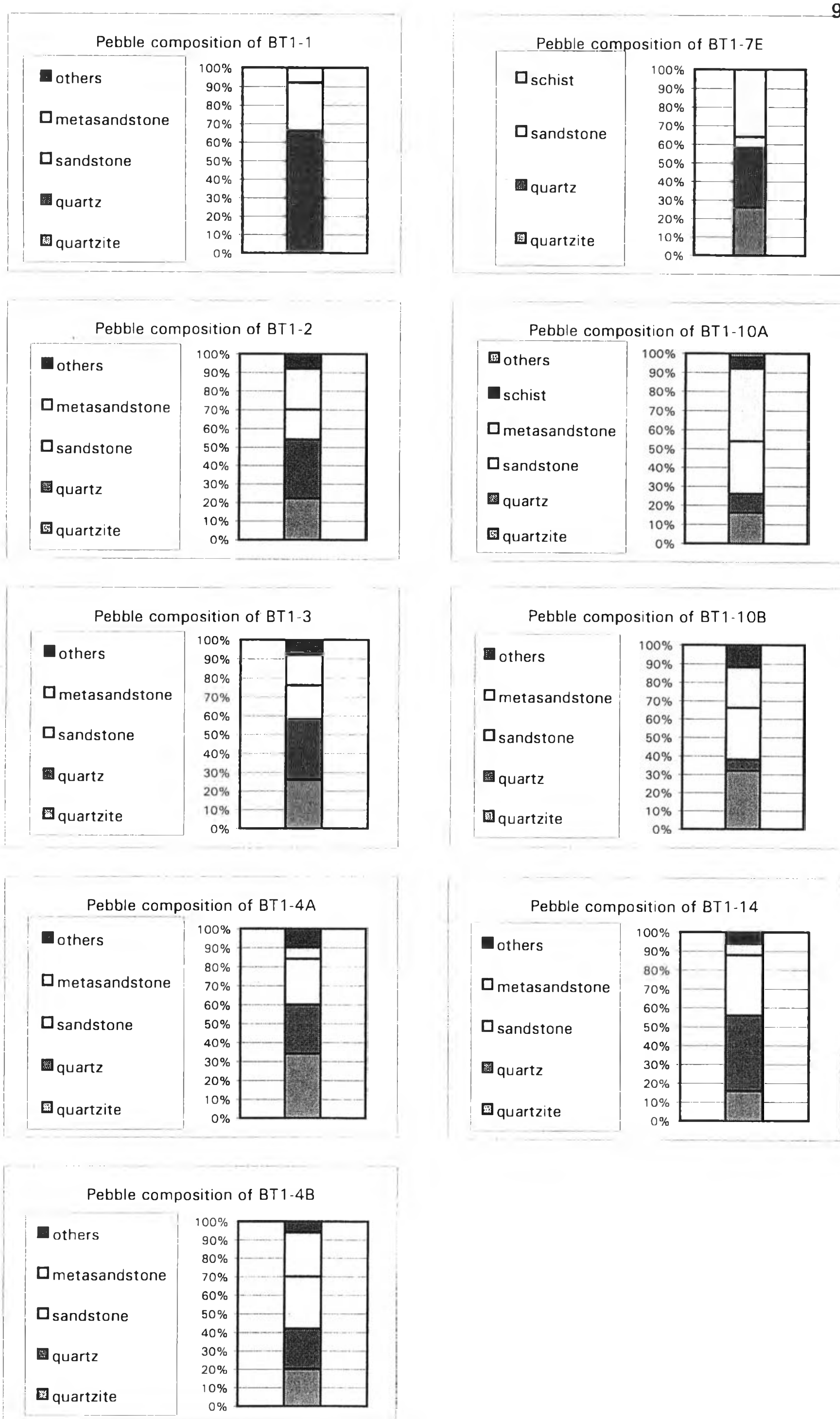

Figure 5.14 Gravel composition of Ban Tak Tertiary landform unit.

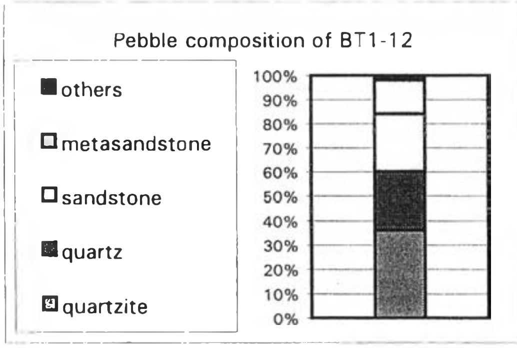

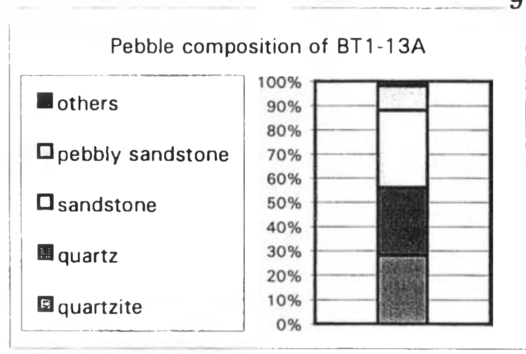

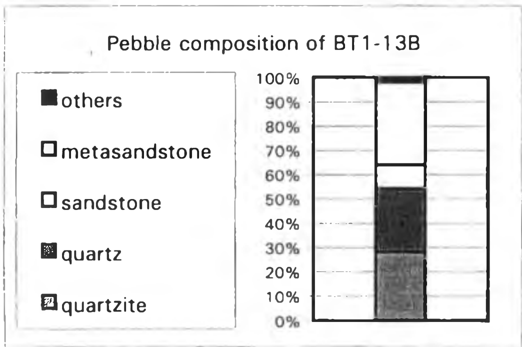

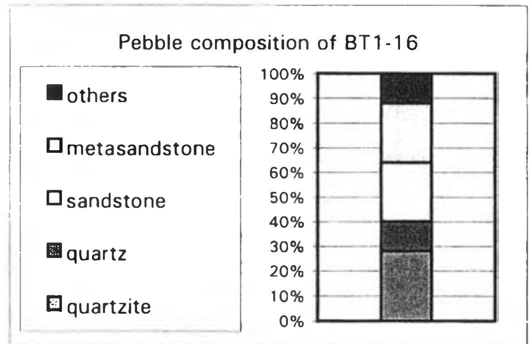

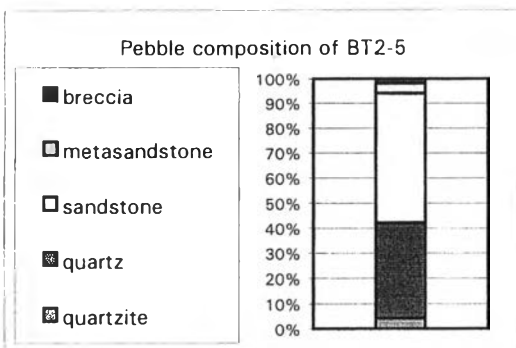

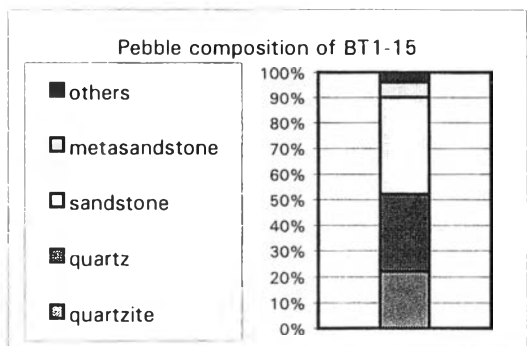

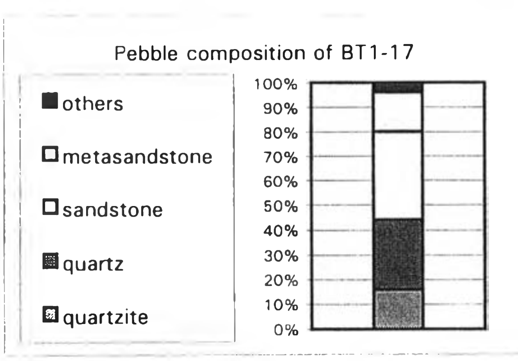

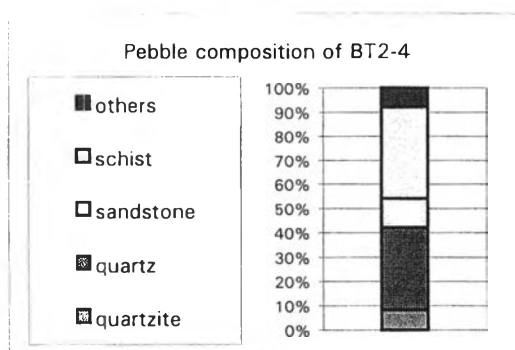

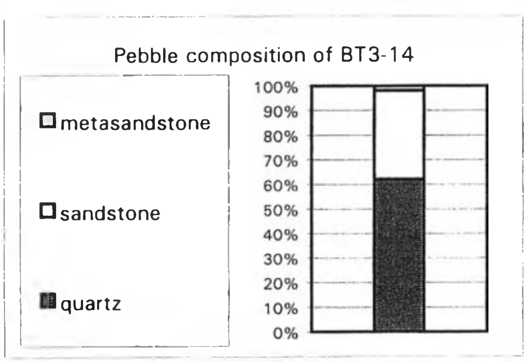

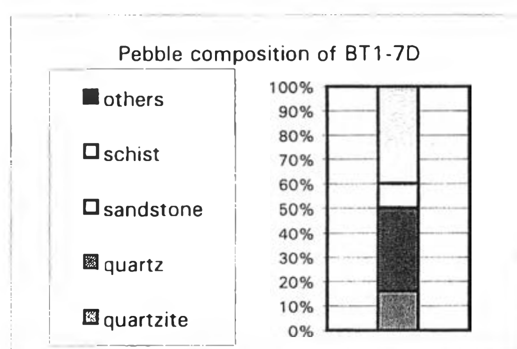

Figure 5.15 Gravel composition of Ban Tak Tertiary landform unit.(cont.)

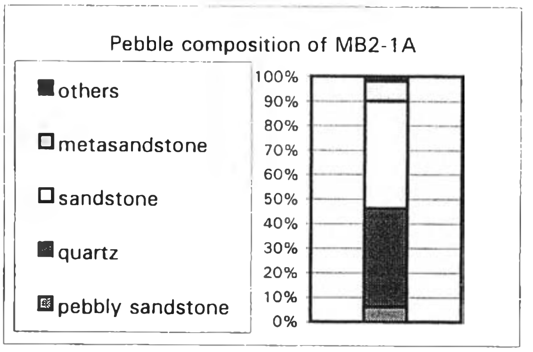

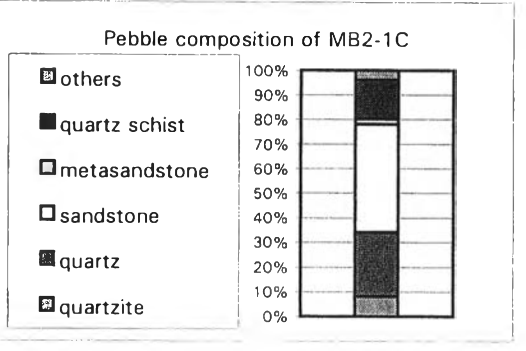

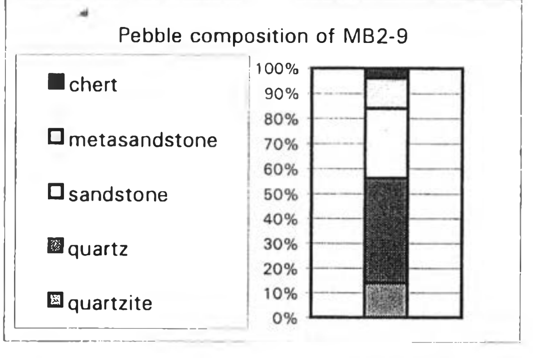

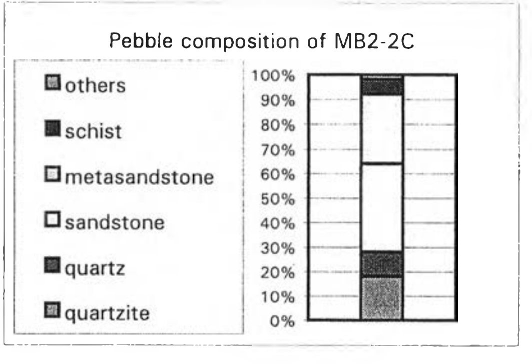

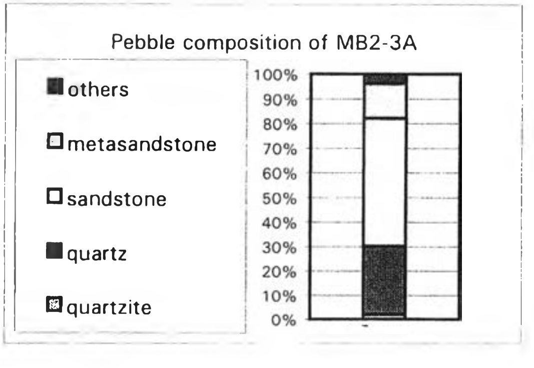

Figure 5.16 Gravel composition of Mae Bon Tertiary landform unit.

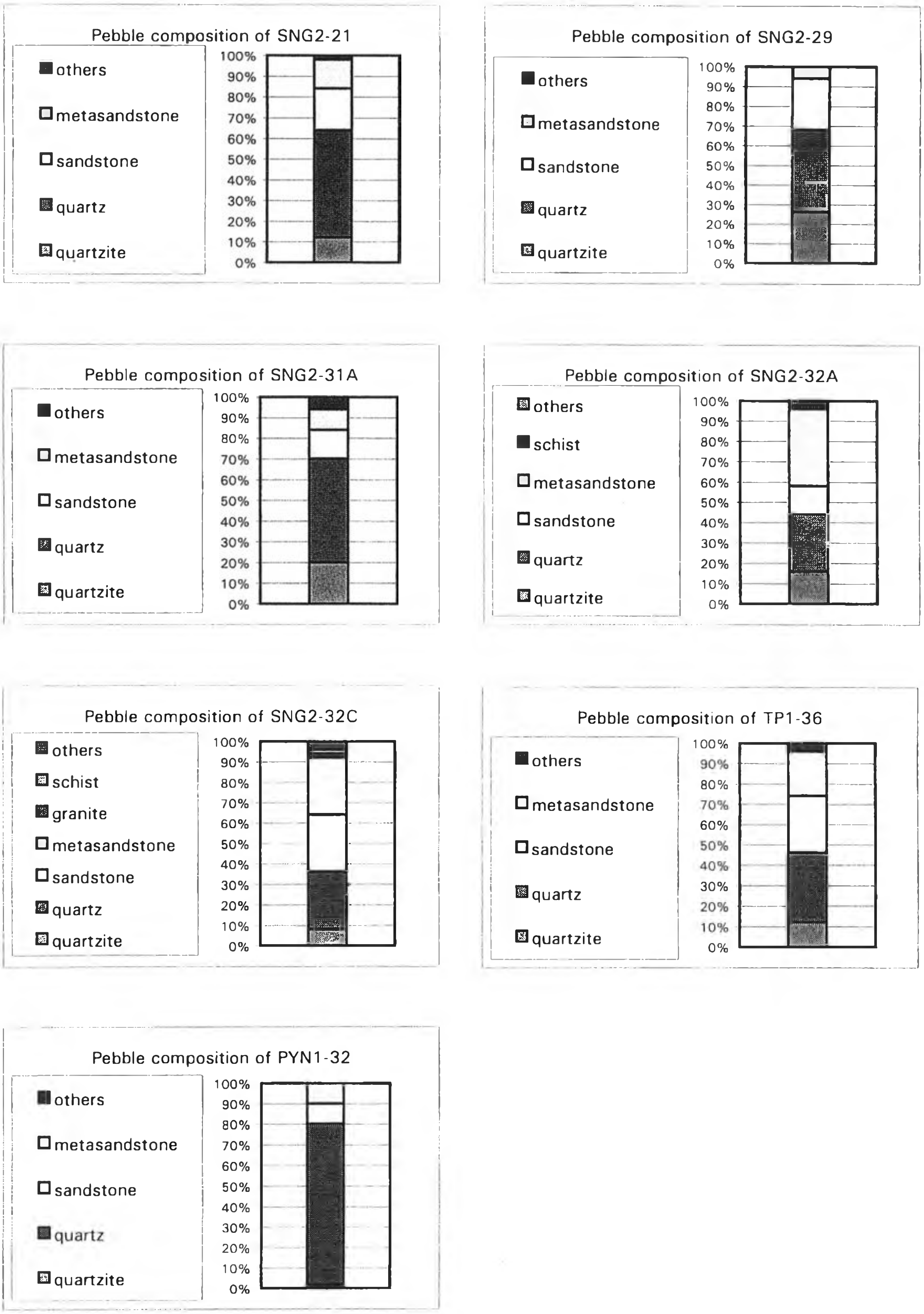

Figure 5.17 Gravel composition of Sam Ngao (SNG2-21, SNG2-29, SNG2-31A, SNG2-32A, and SNG2-32C), Tha Pui (TP1-36) and Pa Yang Nua (PYN1-32) high terrace.

is composed of quartzite, quartz, sandstone and metasandstone, in contrast, the minor component of Mae Salid high terrace is schist, tuff, volcanic breccia, pebbly sandstone, tuffaceous sandstone, metatuff, granite and rhyolite. This minor component commonly presents at the lower part of the deposit. Sample no. MS2-20 shows great component of tuff up to about 60%. It is quite possible that the lower part of the deposit of this terrace has been filled by sediment transported from the ancient Wang. Their sources come from volcanic rocks in the north of the area and are brought down by the Wang River.

Figures 5.19 and 5.20 represent the gravel composition of the middle terrace group. That Khunram middle terrace contains locally schist pebbles in the lower part of the deposit. They are assumed to have supplied by schist of upstream Silurian-Devonian rocks in the vicinity area. The content of quartz increases gradually from less than 30 % at That Khunram middle terrace (Figure 5.20) to greater than 60 % at the Pa Yang Tai middle terrace (Figure 5.19). Quartz of samples no. PYT1-30, PYT1-31, and PYT1-26 is expected to have transported from quartz dyke scatter presented upstream.

The gravel composition of the low terrace is shown in Figure 5.21. The components are partly similar to Tertiary landform unit. The content of quartz increases rapidly from some 20-30 % at Ban Mai low terrace, to more than 80 % at Ban Mae Payuap low terrace. Here the strong influence of upstream quartz dyke is obvious. The quartz content of samples no. MP3-10 and MP2-37 can also be assumed that it has been supplied from upstream quartz dyke in the middle part of the area. However, At Ban Pak Thang low terrace, outcrop is not available.

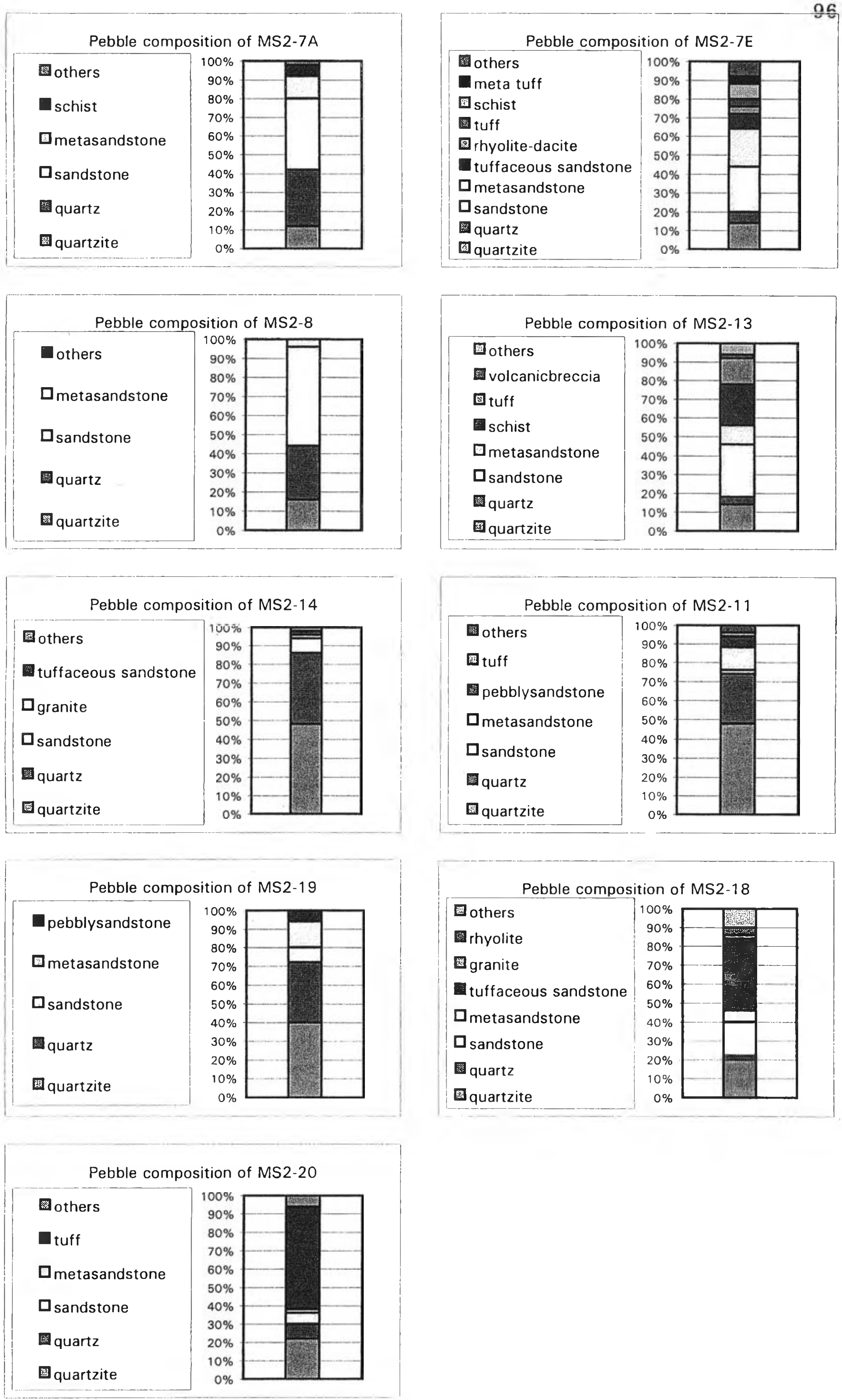

Figure 5.18 Gravel composition of Mae Salid high terrace.

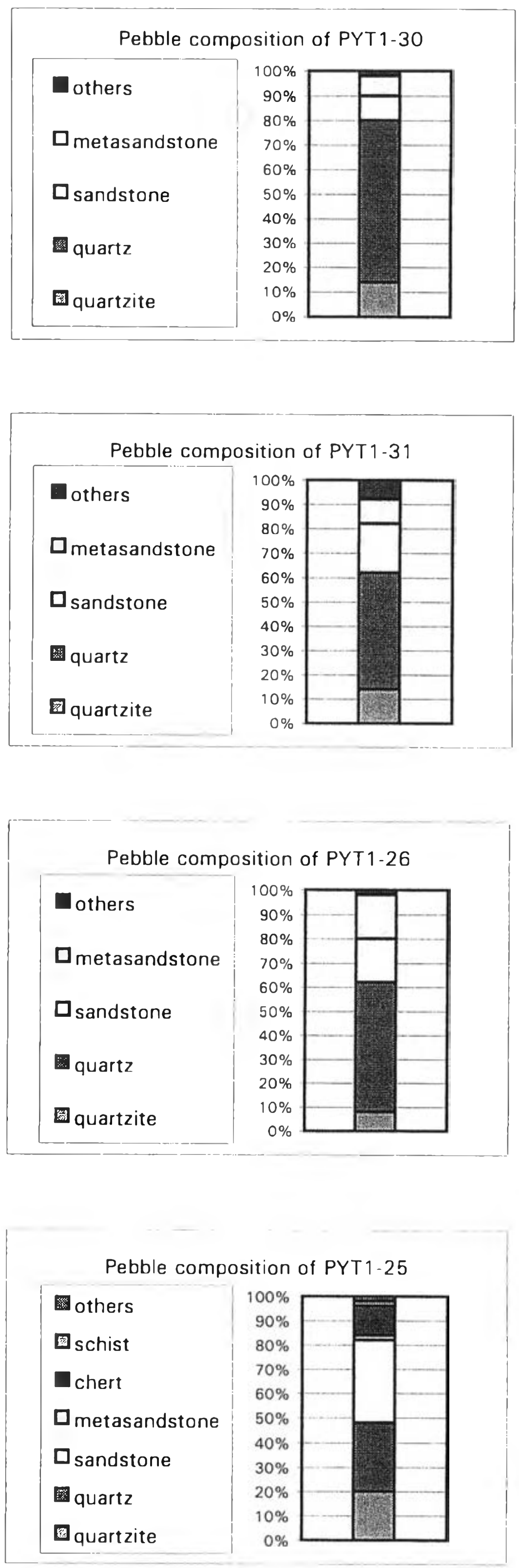

Figure 5.19 Gravel composition of the Pa Yang Tai middle terrace.

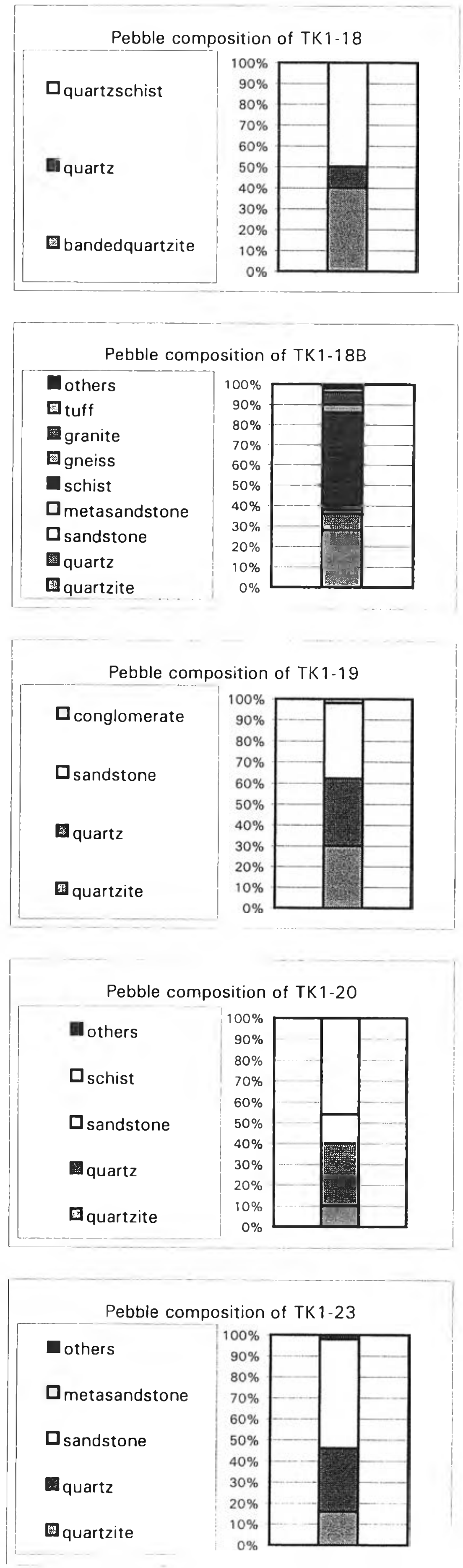

Figure 5.20 Gravel composition of That Khunram middle terrace.

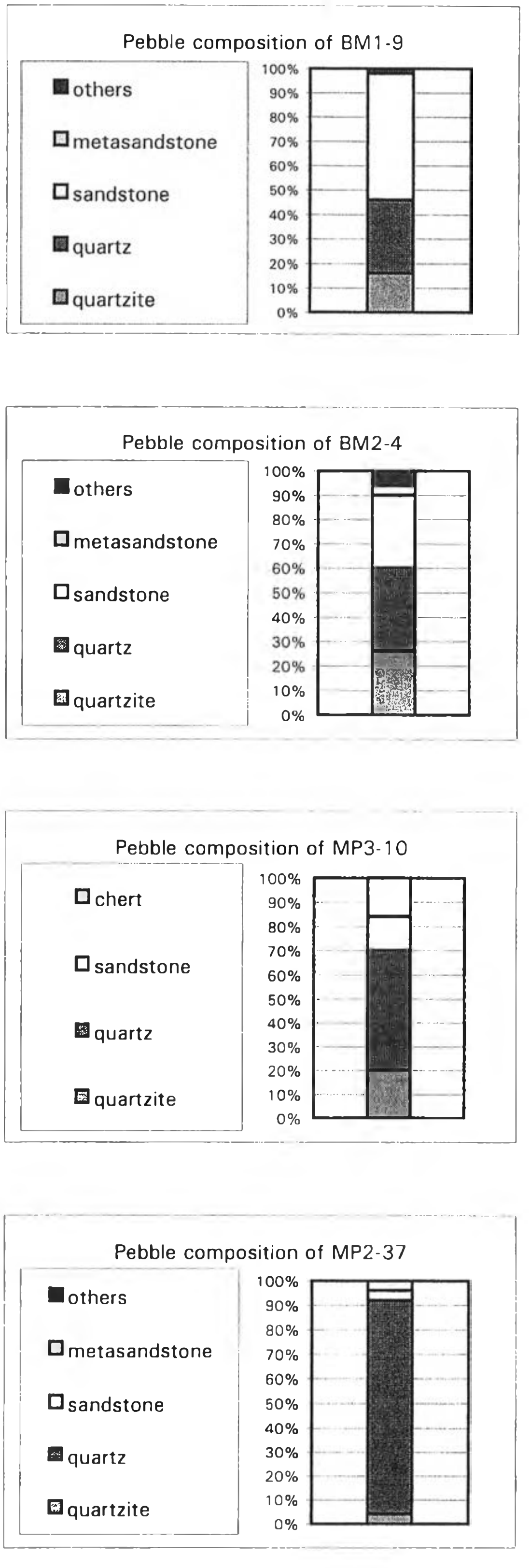

Figure 5.21 Gravel composition of Ban Mai low terrace (BM1-9 and BM2-4) and Mae Payuap low terrace(MP3-10 and MP2-37).

Grain size distribution

Result for grain size analyses by sieving and hydrometer tests is illustrated in the form of histograms, the two kinds of cumulative graphs and statistic parameters. In the study area, the major sources of river sand are gneiss and quartzschist, which supplied the large amount of quartz sand and some mica. In the fieldwork, 14 drilled holes by hand auger and surface sampling were carried out. Location of auger holes for grain size analysis is shown in Figure 5.1. 72 representative samples were collected from the study area in order to confirm their deposition environment. All samples were collected from floodplain unit, natural levee unit, point bar unit and sand bar unit.

Floodplain unit

Figure 5.22 shows some sections of floodplain unit in the study area. 45 samples from 10 drilled holes of floodplain unit were sampling for particle size analysis. Overbank floodplain deposits including all sediments deposited during the flood above the channel and bank sediments.

Figure 5.23 shows histograms of size distribution from auger hole no. FP3-1. At the top of the deposits, they are sandy clay silt (samples no. FP3-1A and B). The content of silt fractions is 48 to 45% and clay particle are up to 26 and 33 %, respectively. They contain very fine sand up to 12%. Sample no. FP3-1C is silty clay sand, which composed maximum percent of very fine sand up to 26 %, silt content up to 37 % and clay content up to 25 %. The lower part of the deposits is composed of silty clay layers (samples no. FP3-1D, E, and F). They show percent of clay content > 47. Histogram of size distribution from auger hole no. FP3-2 is shown in Figure 5.24. The deposits contain large amount of sand fractions. They are silty sand at the top of the deposits (samples no. FP3-2A). These sand fractions show maximum percent in medium sand. Samples no. FP3-2B, C, D, E, and F are silty clay sand. The maximum percent of sand fractions is very fine sand. Silt fractions range between 19 to 33 % and clay fractions range between 15 to 25 %. It can be note that the clay fractions are present at the down hole.

In Figure 5.25, sand fractions are dominant. Samples from auger hole no. FP3-6 from top to bottom are silty clay sand (sample no. FP3-6A), pebbly sand (samples no. FP3-6B and C), and silty sand (sample no. FP3-6D). Samples from auger hole no. FP3-

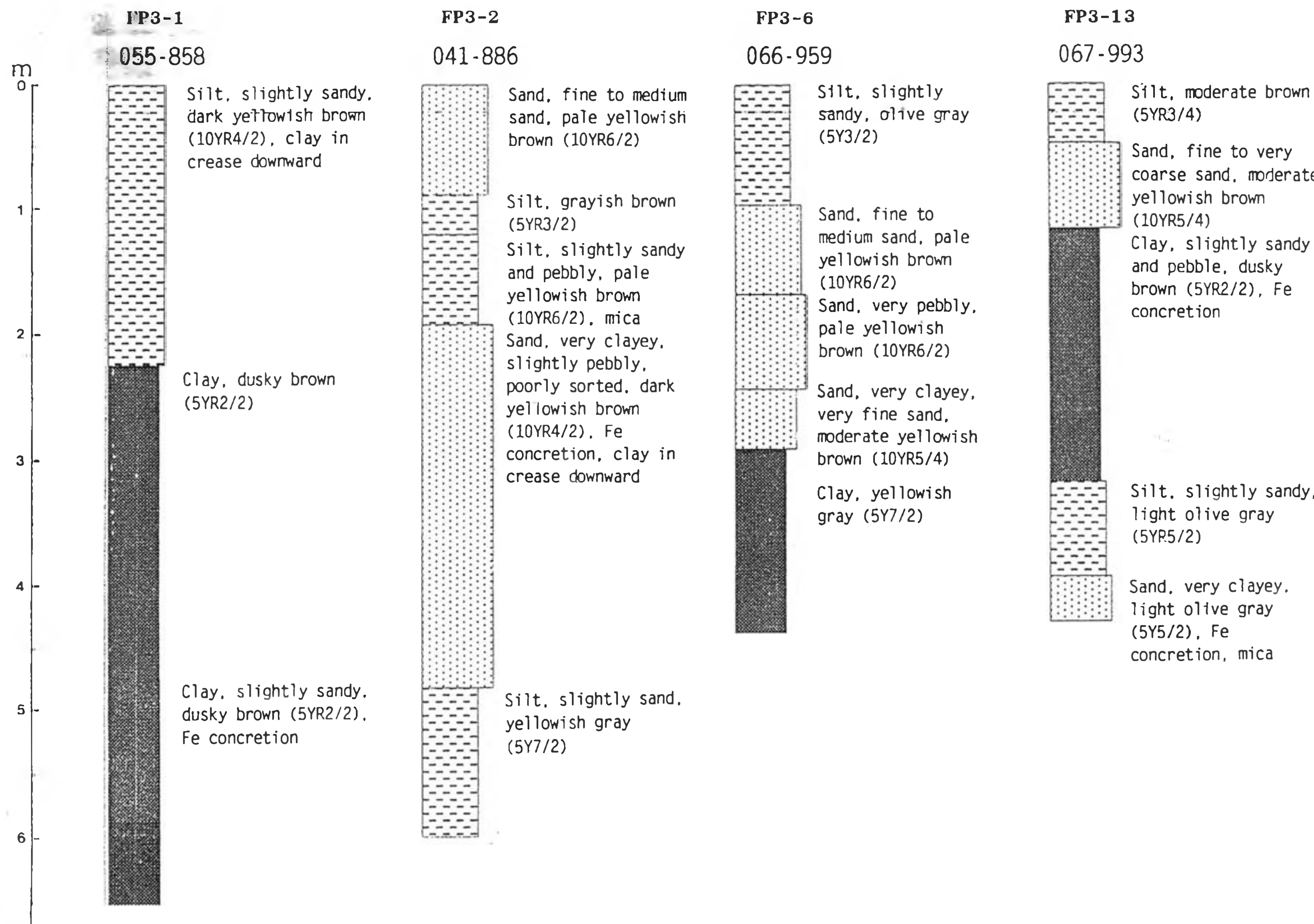

Figure 5.22 Sections in floodplain unit.

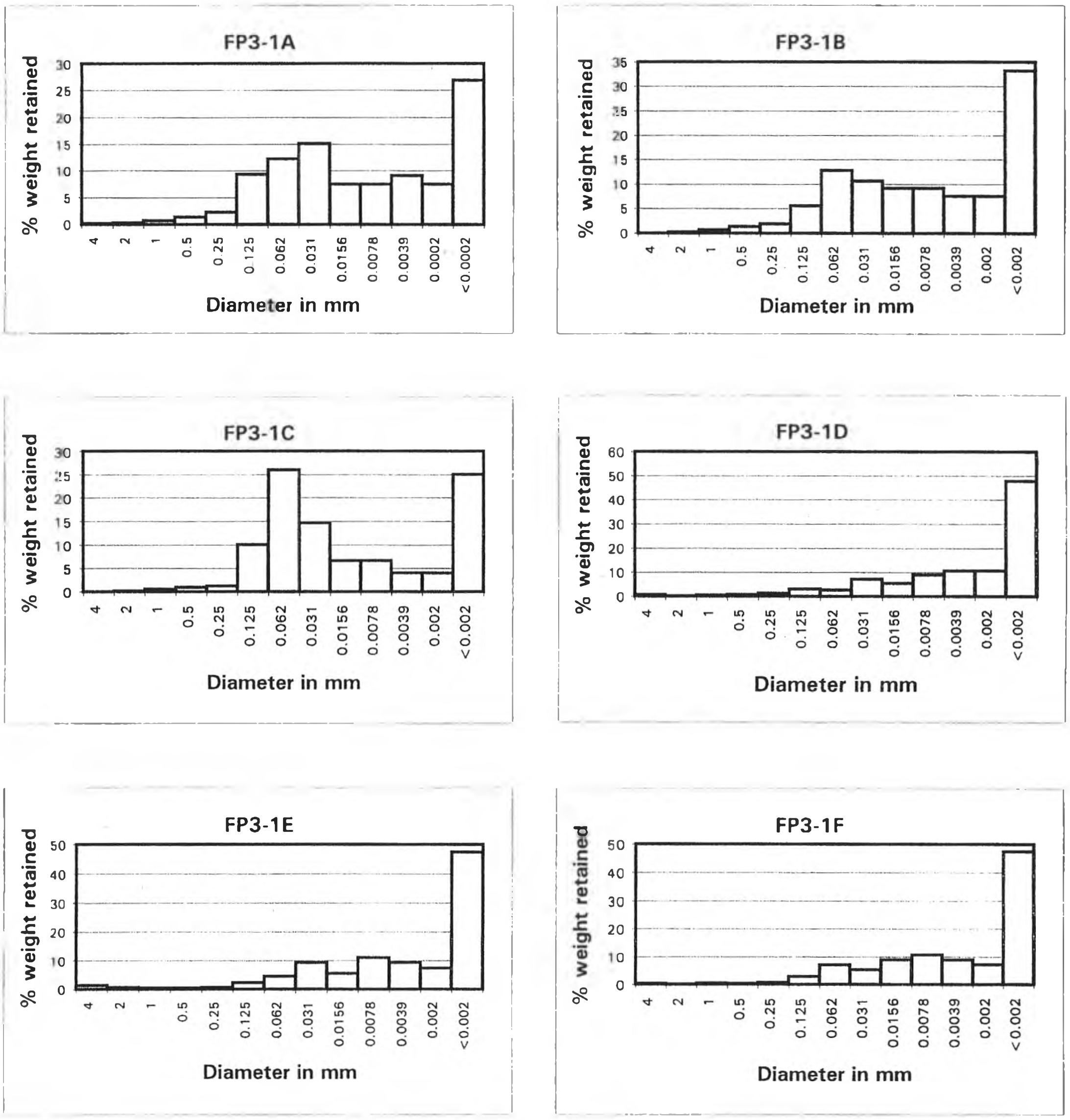

Figure 5.23 Histogram of size distribution from auger hole no. FP3-1.

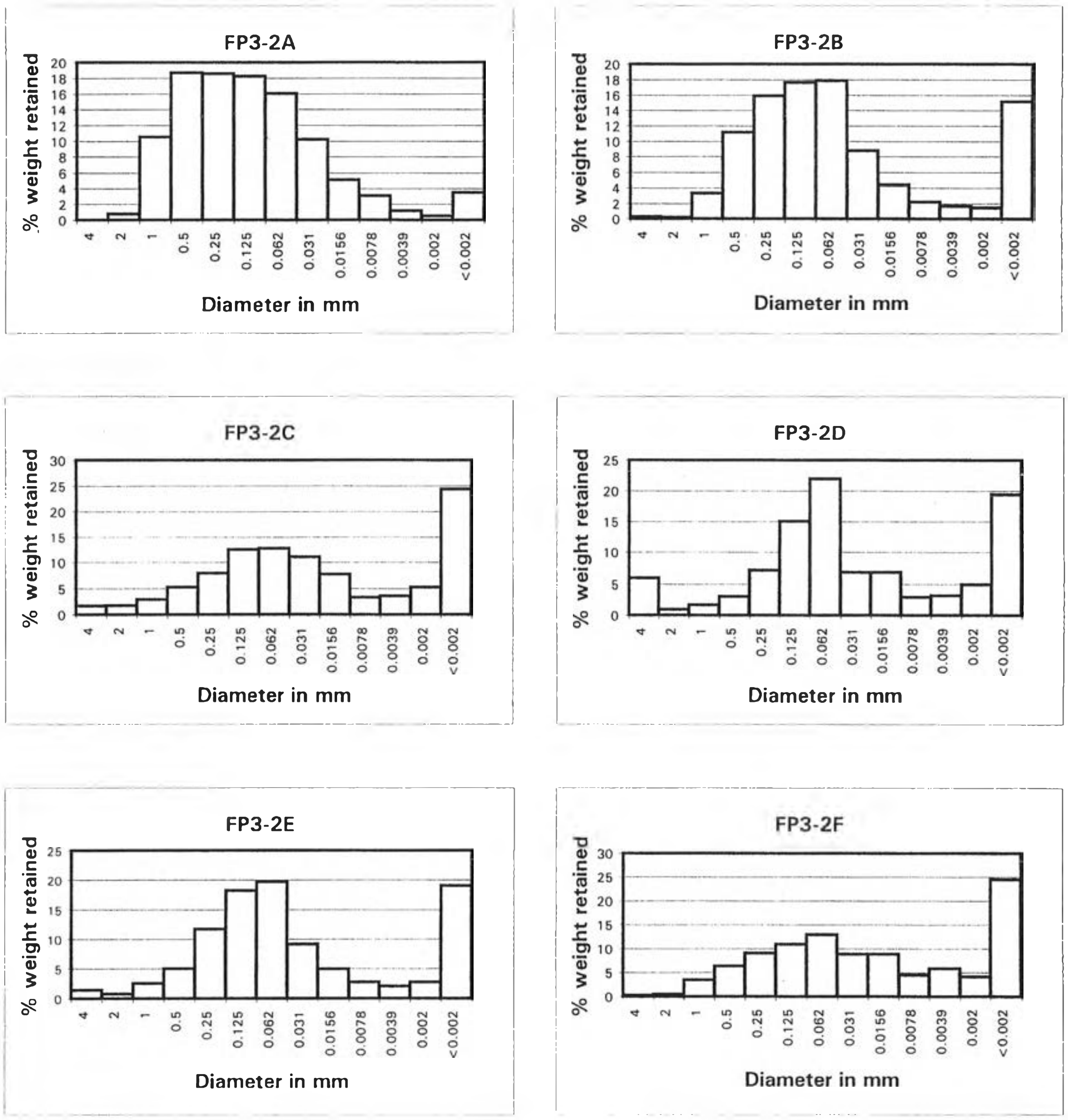

Figure 5.24 Histogram of size distribution from auger hole no. FP3-2.

13 show sandy clay silt (samples no. FP3-13A and C) alternate with pebbly sand. Sample no. FP3-13D is sandy silty clay, which contains clay fractions up to 50 %. The lower part of the deposits show silty clay sand (sample no. FP3-13E) and underlying silty sand (samples no. FP3-13F).

In some places, samples from floodplain unit are composed of high content of sand fractions. Figures 5.26, 5.27, and 5.28 show samples that contain sand fractions dominant. Samples from the upper part of auger hole no. FP-3 show maximum percent of sand fractions range from fine to medium (samples no. FP-3A, B, C, and D). At the bottom of auger hole no. FP-3, sample no. FP-3E and F are pebbly sand. From auger hole no. FP3-3, the deposits from top to bottom are composed of silty sand, silty clay sand (sample no. FP3-3A and B) underlain by sandy clay silt (sample no. FP3-3C).

Figure 5.27 shows samples from auger holes no. FP2-25 and FP2-23. Auger hole no. FP2-25 contains silty sand at the top of the deposits (samples no. FP2-25A). It underlain by pebbly sand that shows maximum percent of very fine to fine pebble range from 38 to 55 % (samples no. FP2-25B, C, and D). For samples from auger hole no. FP2-23, it can be note that size fractions in this hole can be correlated to the hole no. FP2-25. It consists samples show silty clay sand at the top (sample no. FP2-23A) and pebbly sand at the bottom (samples FP2-23B and C).

Figure 5.28 shows samples form auger holes no. FP-6 and FP2-35. Samples from auger hole no. FP-6 are sand which show maximum percent of coarse sand up to 26 at the top of the deposits (sample no. FP-6A) and very coarse sand at the bottom (sample no. FP-6B). Samples from auger hole no. FP2-35 are mainly composed of pebbly sand which show maximum percent of sand fractions range between fine to coarse (samples no. FP2-35A, B, D, and E). These pebbly sand are alternate by silty clay sand (sample no. FP2-35C).

In Figure 5.29-above, the curves represent the frequency of grain size samples from floodplain. From these curves, some of samples show bi-modal character of two maximum size classes. This bi-modal character of the sediment is able to point out the deposition from river with large seasonal variations in stream capacity and velocity (Nossin, 1959). The statistic values of the sediments from cumulative frequency curves (Figure 5.29-below) are presented in Tables 5.2-5.5.

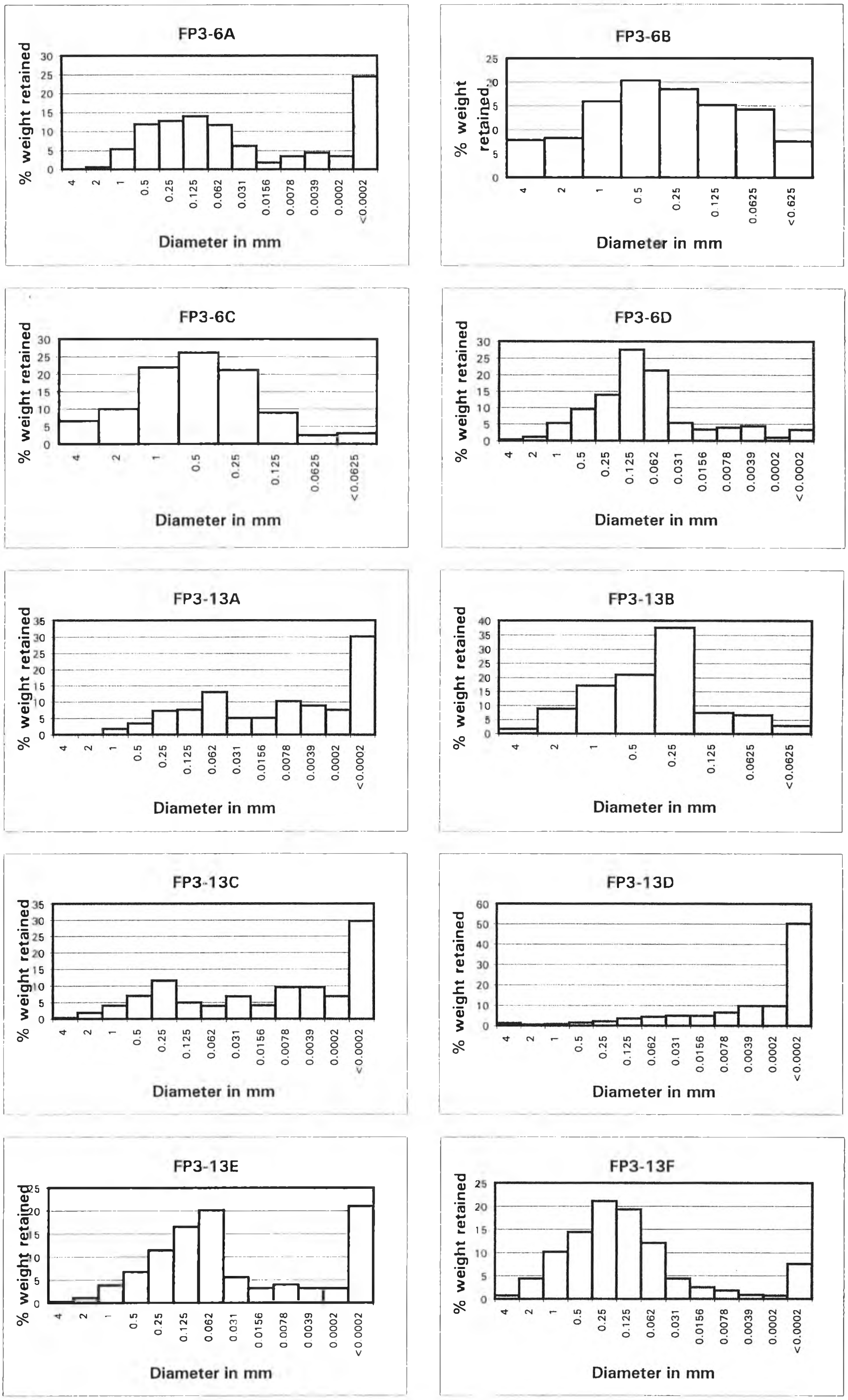

Figure 5.25 Histogram of size distribution from auger hole no. FP3-6 and FP3-13.

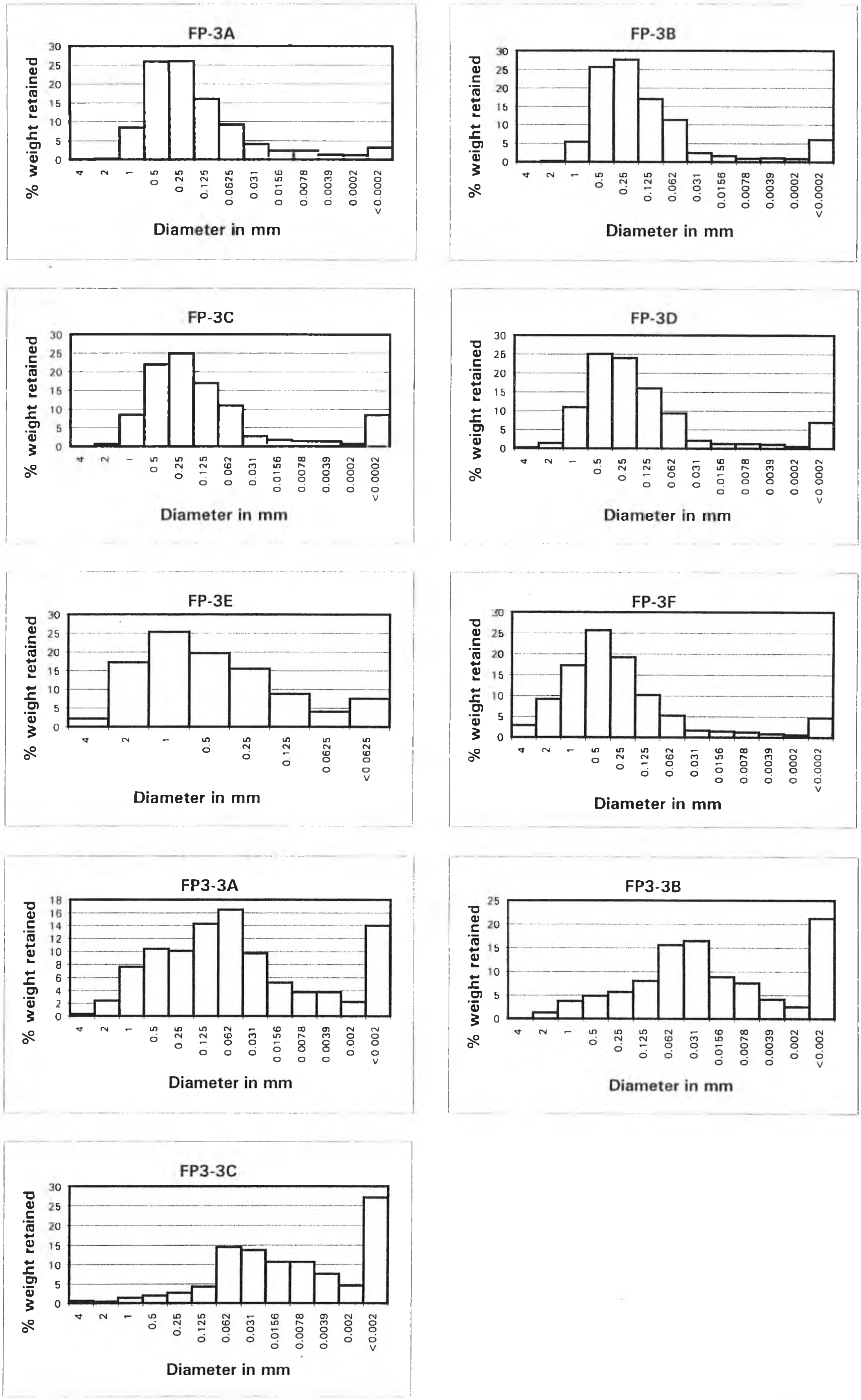

Figure 5.26 Histogram of size distribution from auger hole no. FP-3 and FP3-3.

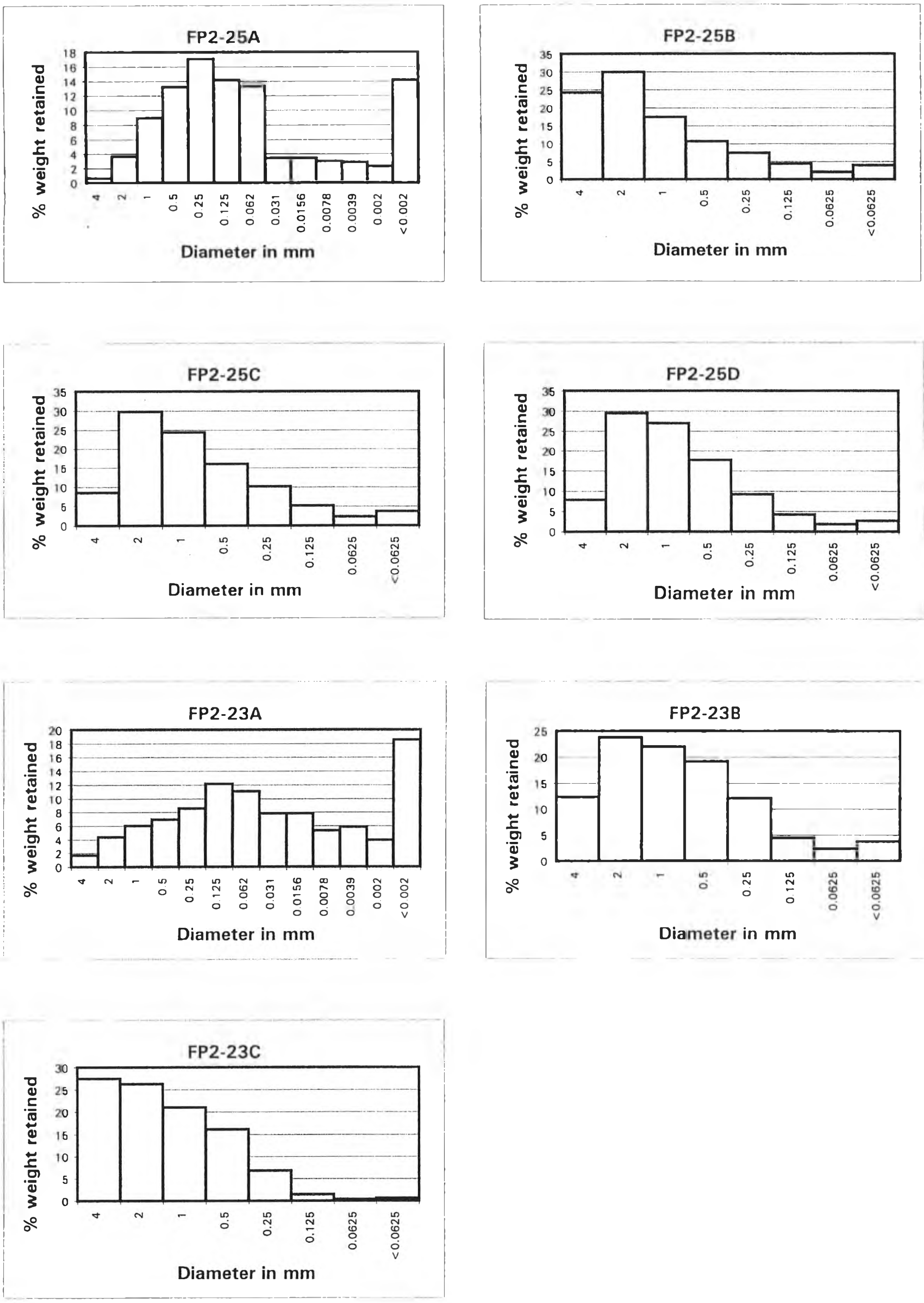

Figure 5.27 Histogram of size distribution from auger hole no. FP2-25 and FP2-23.

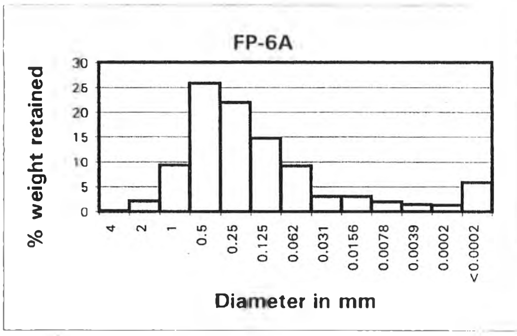

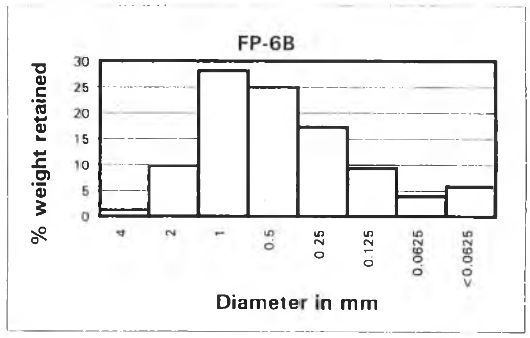

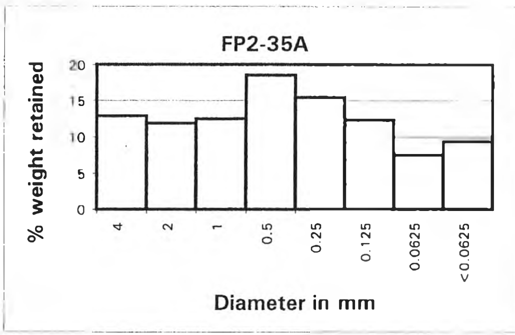

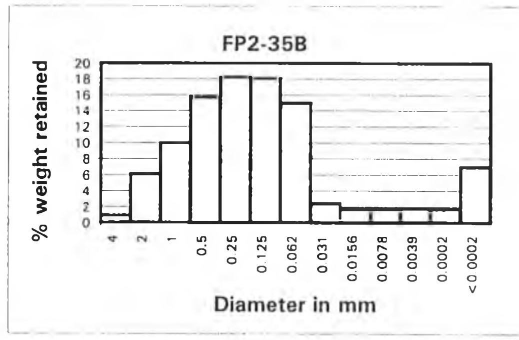

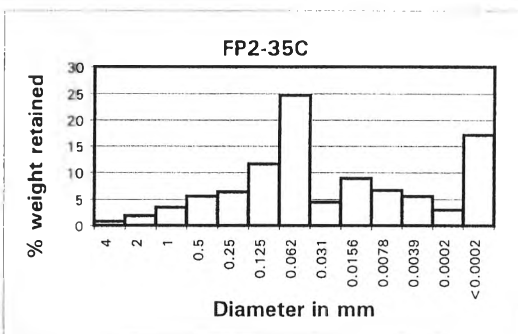

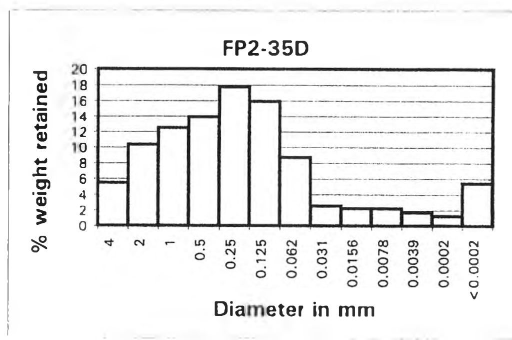

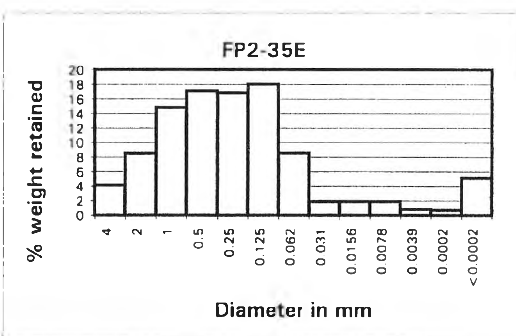

Figure 5.28 Histogram of size distribution from auger hole no. FP-6 and FP2-35.

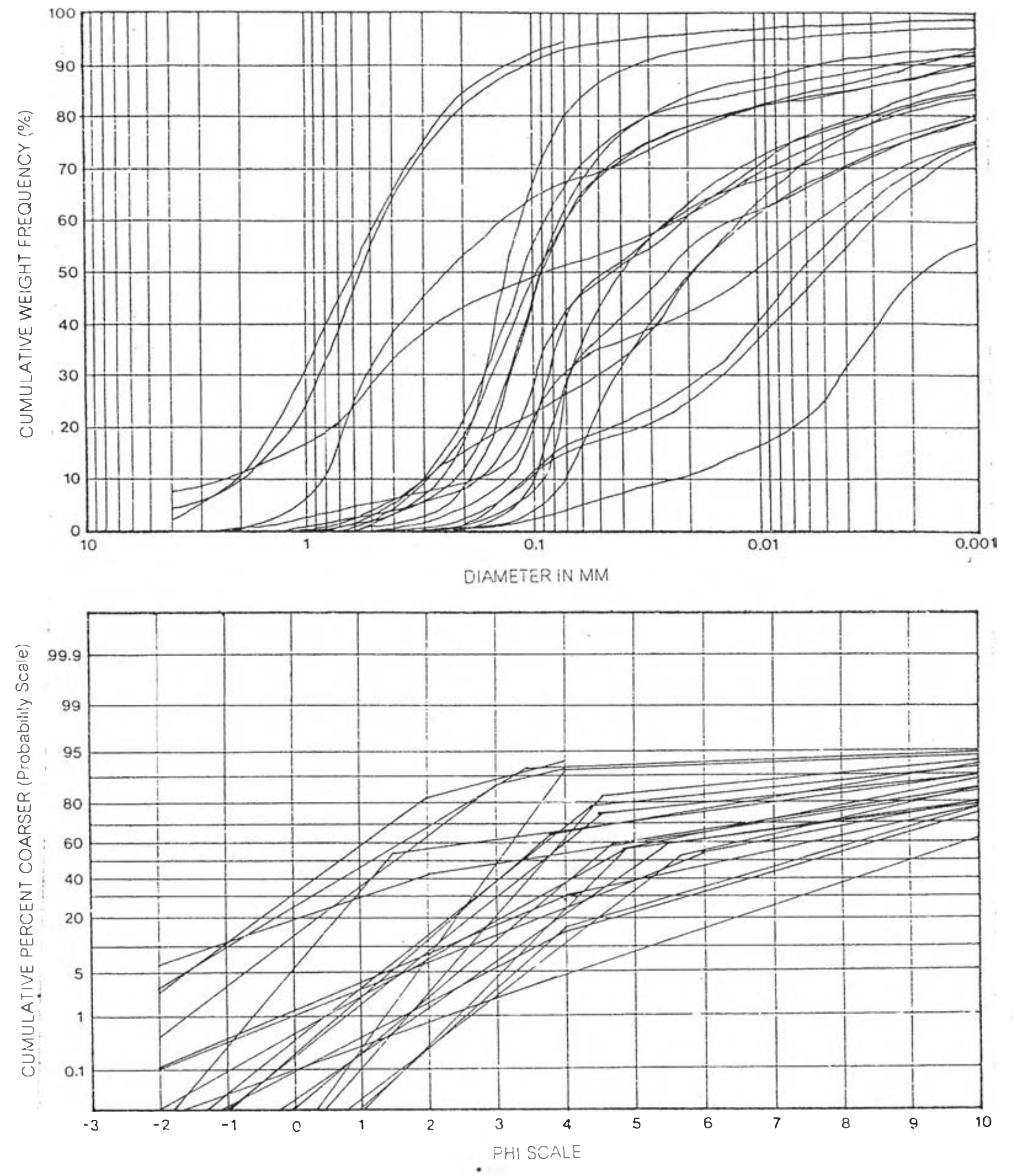

Figure 5.29 Two types of compilation plots of samples from floodplain unit. S-curve when using arithmetic ordinate scale cumulative against log-scale of diameters (above) and most of curves when plot by using probability cumulative against diameters in phi scale (below).

Table 5.2 Size distribution of samples from floodplain unit compare with standard phi mean from Friedman and Sander, 1978.

Sample	Values of mean	Size
FP-3A	2.25	fine sand
FP-3B	1.82	medium sand
FP-3C	2.58	fine sand
FP-3D	1.83	medium sand
FP-3E	0.58	coarse sand
FP-3F	1.33	medium sand
FP2-23A	4.92	very coarse silt
FP2-23B	-0.10	very coarse sand
FP2-23C	-1.03	very fine pebbles
FP2-25A	4.08	very coarse silt
FP2-25B	-1.38	very fine pebbles
FP2-25C	-0.42	very coarse sand
FP2-25D	-0.55	very coarse sand
FP3-1A	6.88	medium silt
FP3-1B	7.50	fine silt
FP3-1C	6.67	medium silt
FP3-1D	9.47	clay
FP3-1E	8.65	very fine silt
FP3-1F	8.35	very fine silt
FP3-2A	2.67	fine sand
FP3-2B	4.57	very coarse silt
FP3-2C	5.67	coarse silt
FP3-2D	5.22	coarse silt
FP3-2E	5.13	coarse silt
FP3-2F	5.88	coarse silt
FP3-3A	4.23	very coarse silt
FP3-3B	5.95	coarse silt
FP3-3C	6.73	medium silt
FP3-6A	6.32	medium silt
FP3-6B	1.00	medium sand
FP3-6C	0.50	coarse sand
FP3-6D	3.08	very fine sand
FP3-13A	7.03	fine silt
FP3-13B	0.72	coarse sand
FP3-13C	6.67	midium silt
FP3-13D	9.60	clay
FP3-13E	5.50	coarse silt
FP3-13F	2.08	fine sand
FP2-35A	0.88	coarse sand
FP2-35B	2.30	fine sand
FP2-35C	5.17	coarse silt
FP2-35D	1.53	medium sand
FP2-35E	1.30	medium sand
FP-6A	2.30	fine sand
FP-6B	0.68	coarse sand

Table 5.3 Comparison of sand samples from floodplain unit based on sorting values, compare with standard sorting term of Briggs (1977).

Sample	Values of sorting	Sorting class
FP-3A	1.93	poorly sorted
FP-3B	1.65	poorly sorted
FP-3C	2.12	very poorly sorted
FP-3D	1.92	poorly sorted
FP-3E	1.79	poorly sorted
FP-3F	2.23	very poorly sorted
FP2-23A	4.45	extremely poorly sorted
FP2-23B	1.64	poorly sorted
FP2-23C	1.47	poorly sorted
FP2-25A	3.66	very poorly sorted
FP2-25B	2.57	very poorly sorted
FP2-25C	1.89	poorly sorted
FP2-25D	1.26	poorly sorted
FP3-1A	3.74	very poorly sorted
FP3-1B	4.11	extremely poorly sorted
FP3-1C	4.36	extremely poorly sorted
FP3-1D	4.91	extremely poorly sorted
FP3-1E	3.57	very poorly sorted
FP3-1F	3.04	very poorly sorted
FP3-2A	2.41	very poorly sorted
FP3-2B	3.33	very poorly sorted
FP3-2C	4.75	extremely poorly sorted
FP3-2D	4.01	extremely poorly sorted
FP3-2E	4.30	extremely poorly sorted
FP3-2F	4.42	extremely poorly sorted
FP3-3A	3.77	very poorly sorted
FP3-3B	4.14	extremely poorly sorted
FP3-3C	3.82	very poorly sorted
FP3-6A	6.09	extremely poorly sorted
FP3-6B	1.91	poorly sorted
FP3-6C	1.42	poorly sorted
FP3-6D	2.12	very poorly sorted
FP3-13A	4.58	extremely poorly sorted
FP3-13B	1.25	poorly sorted
FP3-13C	5.32	extremely poorly sorted
FP3-13D	5.03	extremely poorly sorted
FP3-13E	4.74	extremely poorly sorted
FP3-13F	2.53	very poorly sorted
FP2-35A	2.47	very poorly sorted
FP2-35B	2.74	very poorly sorted
FP2-35C	3.80	very poorly sorted
FP2-35D	2.75	very poorly sorted
FP2-35E	2.44	very poorly sorted
FP-6A	2.08	very poorly sorted
FP-6B	1.45	poorly sorted

Table 5.4 Classification of samples from floodplain unit into skewness values described based on standard term by Briggs (1977).

Sample	Values of skewness	Skewness class
FP-3A	0.38	very positive skewed
FP-3B	0.33	very positive skewed
FP-3C	0.63	very positive skewed
FP-3D	0.43	very positive skewed
FP-3E	0.13	positive skewed
FP-3F	0.40	very positive skewed
FP2-23A	0.31	very positive skewed
FP2-23B	0.13	positive skewed
FP2-23C	-0.04	symmetrical
FP2-25A	0.49	very positive skewed
FP2-25B	-0.02	symmetrical
FP2-25C	0.02	positive skewed
FP2-25D	0.04	symmetrical
FP3-1A	0.27	positive skewed
FP3-1B	0.20	positive skewed
FP3-1C	0.58	very positive skewed
FP3-1D	0.02	symmetrical
FP3-1E	-0.03	symmetrical
FP3-1F	0.03	symmetrical
FP3-2A	0.29	positive skewed
FP3-2B	0.53	very positive skewed
FP3-2C	0.44	very positive skewed
FP3-2D	0.49	very positive skewed
FP3-2E	0.44	very positive skewed
FP3-2F	0.24	positive skewed
FP3-3A	0.29	positive skewed
FP3-3B	0.42	very positive skewed
FP3-3C	0.11	positive skewed
FP3-6A	0.71	very positive skewed
FP3-6B	0.04	symmetrical
FP3-6C	0.01	symmetrical
FP3-6D	0.29	positive skewed
FP3-13A	0.19	positive skewed
FP3-13B	0.01	symmetrical
FP3-13C	0.13	positive skewed
FP3-13D	-0.01	symmetrical
FP3-13E	0.53	very positive skewed
FP3-13F	0.25	positive skewed
FP2-35A	0.00	symmetrical
FP2-35B	0.30	very positive skewed
FP2-35C	0.28	positive skewed
FP2-35D	0.18	positive skewed
FP2-35E	0.18	positive skewed
FP-6A	0.48	very positive skewed
FP-6B	0.22	positive skewed

Table 5.5 Classification of samples from floodplain unit into kurtosis description term based on phi scale and compared with standard class of Briggs (1977).

Sample	Values of kurtosis	Kurtosis class
FP-3A	1.80	very leptokurtic
FP-3B	2.02	very leptokurtic
FP-3C	3.20	extremely leptokurtic
FP-3D	2.46	very leptokurtic
FP-3E	1.17	leptokurtic
FP-3F	2.04	very leptokurtic
FP2-23A	0.93	mesokurtic
FP2-23B	1.17	leptokurtic
FP2-23C	0.95	mesokurtic
FP2-25A	1.35	leptokurtic
FP2-25B	1.09	mesokurtic
FP2-25C	1.03	mesokurtic
FP2-25D	1.23	leptokurtic
FP3-1A	0.89	platykurtic
FP3-1B	0.87	platykurtic
FP3-1C	1.14	leptokurtic
FP3-1D	0.94	mesokurtic
FP3-1E	0.94	mesokurtic
FP3-1F	0.95	mesokurtic
FP3-2A	1.45	leptokurtic
FP3-2B	1.35	leptokurtic
FP3-2C	0.96	mesokurtic
FP3-2D	1.05	mesokurtic
FP3-2E	1.24	leptokurtic
FP3-2F	0.88	platykurtic
FP3-3A	1.29	leptokurtic
FP3-3B	1.13	leptokurtic
FP3-3C	0.93	mesokurtic
FP3-6A	1.01	mesokurtic
FP3-6B	1.03	mesokurtic
FP3-6C	0.93	mesokurtic
FP3-6D	1.52	very leptokurtic
FP3-13A	0.87	platykurtic
FP3-13B	1.02	mesokurtic
FP3-13C	0.84	platykurtic
FP3-13D	0.94	mesokurtic
FP3-13E	1.16	leptokurtic
FP3-13F	1.75	very leptokurtic
FP2-35A	0.94	mesokurtic
FP2-35B	1.59	very leptokurtic
FP2-35C	1.11	leptokurtic
FP2-35D	1.40	leptokurtic
FP2-35E	1.43	leptokurtic
FP-6A	2.34	very leptokurtic
FP-6B	1.28	leptokurtic

From the tables, the summary of sediment characteristics of floodplain unit is shown in Table 5.10. It can be divided into 2 parts, lower floodplain and upper floodplain. The lower floodplain, the average means is medium silt. The average degree of sorting (So) is very poorly sorted. Average skewness (Sk) has positive skewed. This means the deposits contain fine particle than coarse particle. Average kurtosis has mesokurtic that means the value close to a normal distribution.

In upper floodplain, the average means is medium sand. The average degree of sorting (So) is very poorly sorted. Average skewness (Sk) has positive skewed. Average kurtosis has very leptokurtic. This means the distribution curve is more peaked than normal.

Natural levee unit

In natural levee unit, 20 samples were collected from 4 drilled holes. Sections of natural levee unit are shown in Figure 5.30. Figure 5.31 shows histograms of size distribution from Wang River (auger hole no. NL2-30) and from Ping River (auger hole no. NL3-2). Samples no NL2-30A, B, and C are sandy clay silt. They are composed of clay fraction up to 26 % and very coarse silt up to 28%. The underlying silty clay (samples no. NL2-30D) contains large amount of clay up to 50 %. Samples from auger hole no. NL3-2 contain sand at the top and the bottom of deposits (sample no. NL3-2A, and C) and alternate silty sand and silty clay sand (sample no. NL3-2B, and C). The sand layers show maximum percent of sand range between very fine to medium.

Histograms of size distribution from auger hole no. NL3-8 is shown in Figure 5.32. The deposits are sandy clay silt at the top (sample no. NL3-8A and B). They contain large amount of silts fraction up to 50 % and clay fractions up to 34 %. At the lower part, the deposits contain pebbly sand (sample no. NL3-8C and E) alternate with silty clay sand (sample no. NL3-8D). Figure 5.33 shows histograms of size distribution from auger hole no. NL-4. Samples from the upper part of the deposits are silty sand (samples no. NL-4A, B, and C). They show maximum % in very fine to fine sand with small amount of clay content (< 17 %). Histograms of samples from the lower part show sandy clay silt (sample no. NL-4E and G) alternate with sand layer, which shows maximum percent of coarse sand (sample no. NL-4F).

In Figure 5.34-above, the curves represent the frequency in size of samples from natural levee. Some of samples also show bi-modal character similar to floodplain. The statistic values of the materials from the cumulative frequency curves (Figure 5.34-below) present in Tables 5.6-5.9.

The summary of sediment characteristics of natural levee unit is shown in Table 5.11. It can be divided into 2 parts, the Ping natural levee and the Wang natural levee. In the Ping natural levee, the average means is very coarse silt. The average degree of sorting (So) is very poorly sorted. Average skewness (Sk) has very positive skewed. Average kurtosis has very leptokurtic. It means the distribution curve is more peaked than normal.

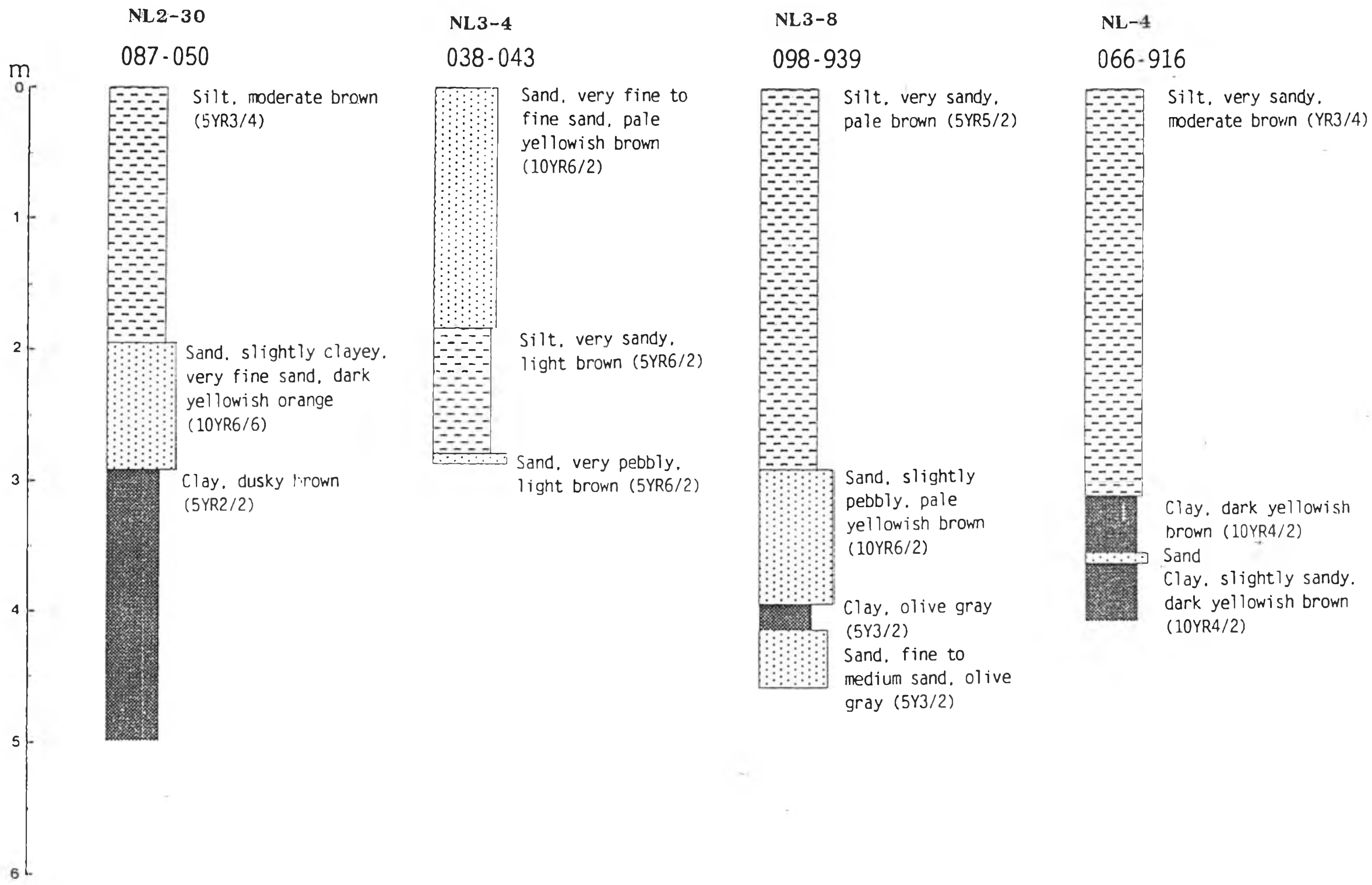

Figure 5.30 Sections in natural levee unit.

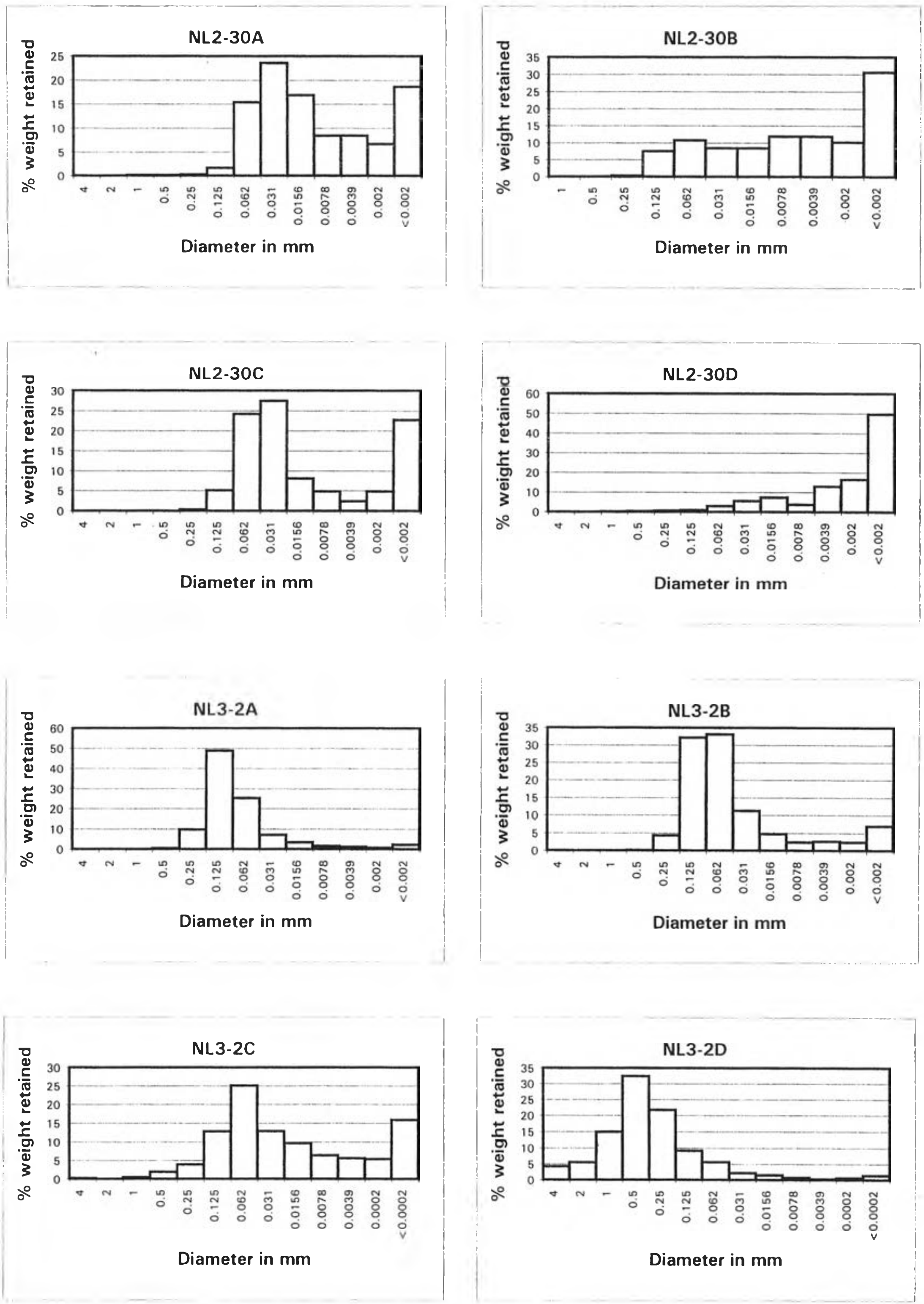

Figure 5.31 Histogram of size distribution from natural levee unit from Wang River (NL2-30) and Ping River (NL3-2) unit.

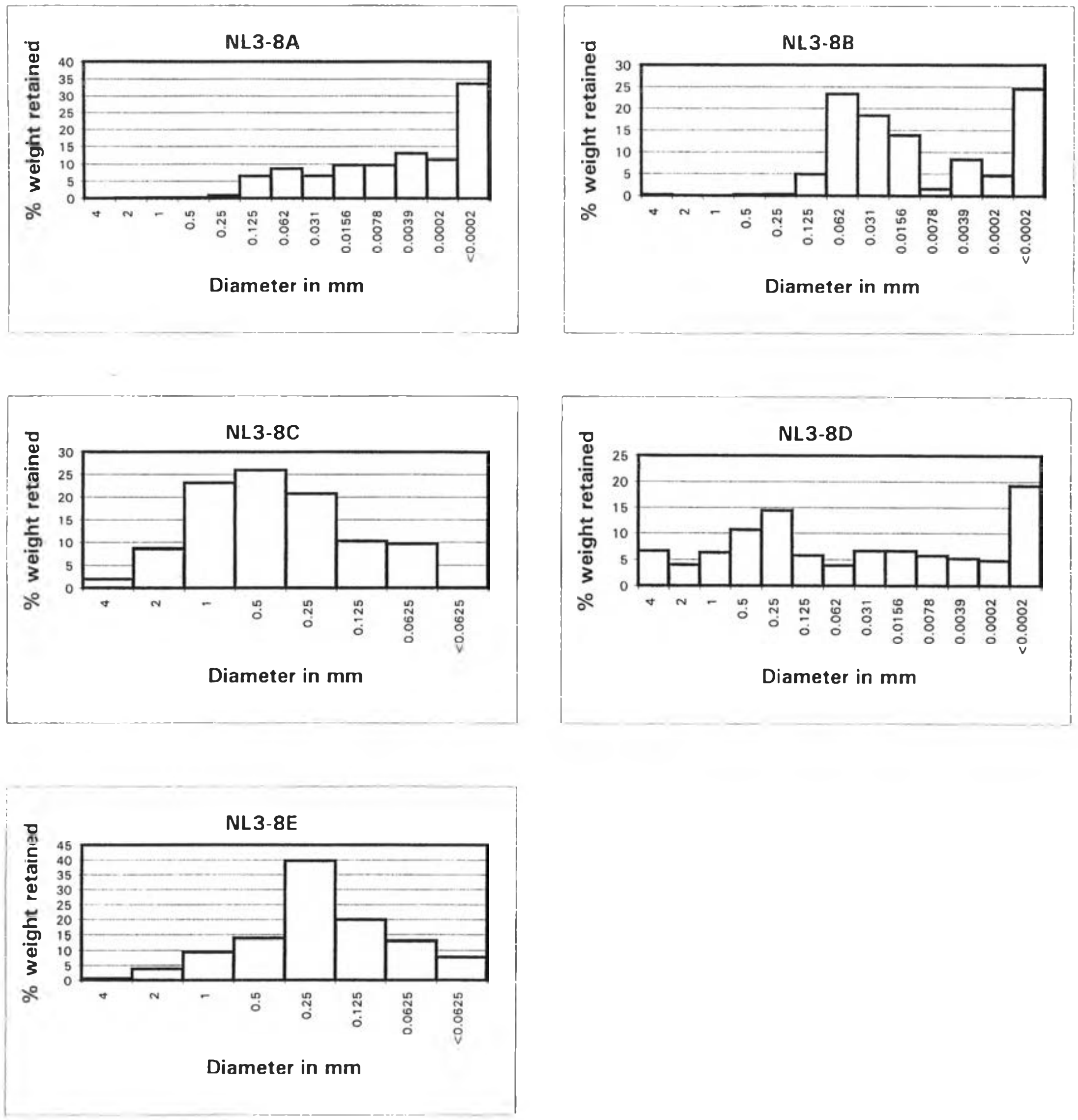

Figure 5.32 Histogram of size distribution from natural levee unit from Wang River.

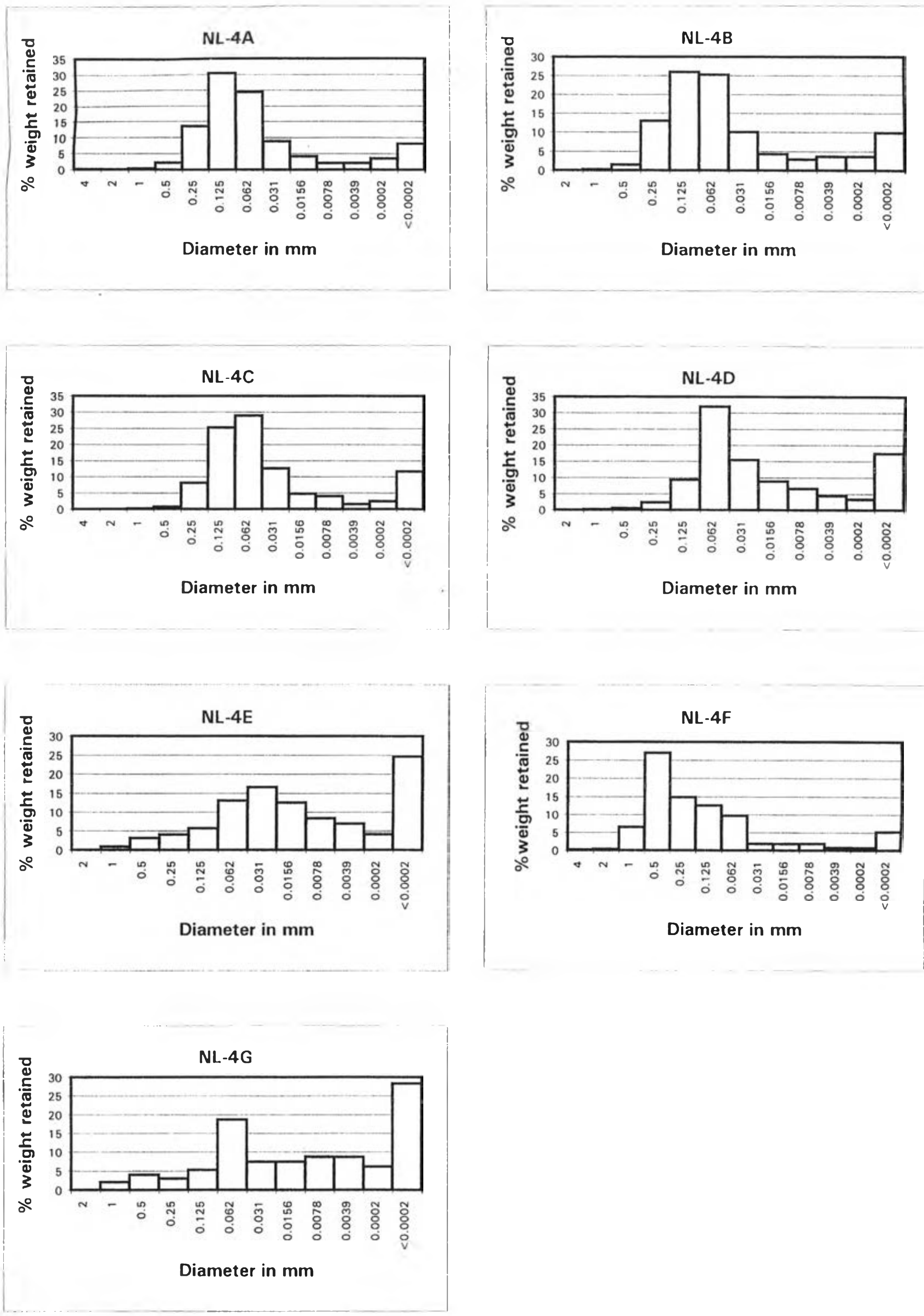

Figure 5.33 Histogram of size distribution from natural levee unit from Ping River shows large amount of fine-very fine sand (A,B,C, and D) alternate with clay(E) and(G), and coarse sand(F)

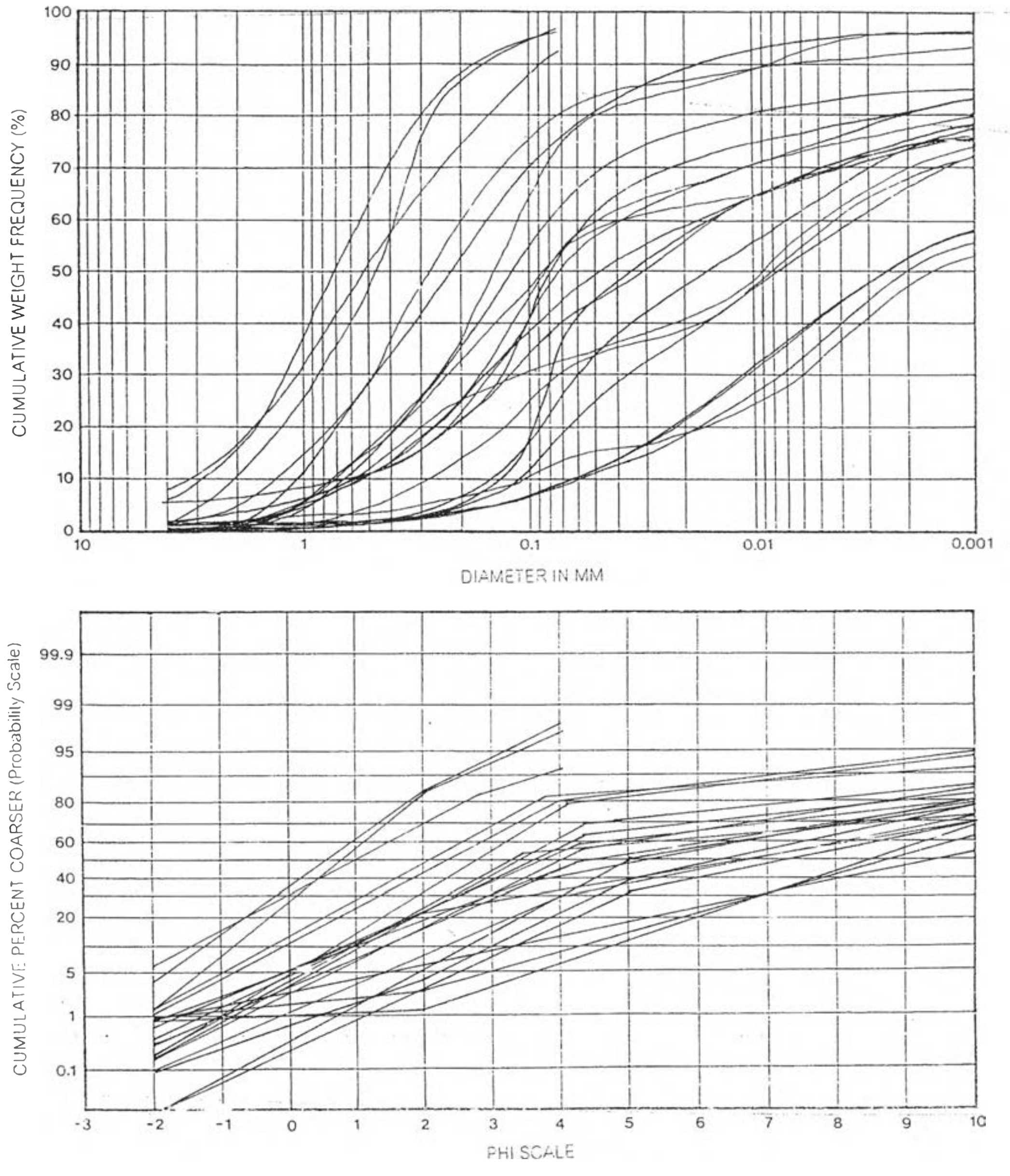

Figure 5.34 Two types of compilation plots of samples from natural levee unit. S-curve when using arithmetic ordinate scale cumulative against log-scale of diameters (above) and most of curves when plot by using probability cumulative against diameters in phi scale (below).

Table 5.6 Size distribution of samples from natural levee unit compare with standard phi mean from Friedman and Sander, 1978.

Sample	Values of mean	Size
NL-4A	4.10	very coarse silt
NL-4B	4.27	very coarse silt
NL-4C	4.67	very coarse silt
NL-4D	5.70	coarse silt
NL-4E	6.50	medium silt
NL-4F	3.33	very fine sand
NL-4G	6.67	medium silt
NL2-30A	6.40	medium silt
NL2-30B	7.40	fine silt
NL2-30C	6.62	medium silt
NL2-30D	9.35	clay
NL3-2A	3.00	very fine sand
NL3-2B	4.00	very coarse silt
NL3-2C	5.45	coarse silt
NL3-2D	1.17	medium sand
NL3-8A	7.65	fine silt
NL3-8B	6.82	medium silt
NL3-8C	0.98	coarse sand
NL3-8D	4.47	very coarse silt
NL3-8E	1.47	medium sand

Table 5.7 Comparison of sand samples from natural levee unit based on sorting values, compare with standard sorting term of Briggs (1977).

Sample	Values of sorting	Sorting class
NL-4A	2.13	very poorly sorted
NL-4B	2.58	very poorly sorted
NL-4C	2.43	very poorly sorted
NL-4D	3.08	very poorly sorted
NL-4E	3.65	very poorly sorted
NL-4F	3.76	very poorly sorted
NL-4G	4.03	extremely poorly sorted
NL2-30A	2.62	very poorly sorted
NL2-30B	3.26	very poorly sorted
NL2-30C	3.66	very poorly sorted
NL2-30D	3.09	very poorly sorted
NL3-2A	0.72	moderately sorted
NL3-2B	1.50	poorly sorted
NL3-2C	3.08	very poorly sorted
NL3-2D	1.72	poorly sorted
NL3-8A	3.42	very poorly sorted
NL3-8B	3.72	very poorly sorted
NL3-8C	1.52	poorly sorted
NL3-8D	5.19	extremely poorly sorted
NL3-8E	1.44	poorly sorted

Table 5.8 Classification of samples from natural levee unit into skewness values described based on standard term by Briggs (1977).

Sample	Values of skewness	Skewness class
NL-4A	0.53	very positive skewed
NL-4B	0.57	very positive skewed
NL-4C	0.55	very positive skewed
NL-4D	0.62	very positive skewed
NL-4E	0.29	positive skewed
NL-4F	0.78	very positive skewed
NL-4G	0.17	positive skewed
NL2-30A	0.51	very positive skewed
NL2-30B	0.07	symmetrical
NL2-30C	0.72	very positive skewed
NL2-30D	0.01	symmetrical
NL3-2A	0.00	symmetrical
NL3-2B	0.41	very positive skewed
NL3-2C	0.42	very positive skewed
NL3-2D	0.02	symmetrical
NL3-8A	0.02	symmetrical
NL3-8B	0.61	very positive skewed
NL3-8C	0.25	positive skewed
NL3-8D	0.29	positive skewed
NL3-8E	0.04	symmetrical

Table 5.9 Classification of samples from natural levee unit into kurtosis description term based on phi scale and compared with standard class of Briggs (1977).

Sample	Values of kurtosis	Kurtosis class
NL-4A	2.06	very leptokurtic
NL-4B	1.29	leptokurtic
NL-4C	2.38	very leptokurtic
NL-4D	1.07	mesokurtic
NL-4E	1.00	mesokurtic
NL-4F	1.02	mesokurtic
NL-4G	0.86	platykurtic
NL2-30A	0.95	mesokurtic
NL2-30B	0.90	mesokurtic
NL2-30C	1.15	leptokurtic
NL2-30D	0.94	mesokurtic
NL3-2A	0.95	mesokurtic
NL3-2B	2.32	very leptokurtic
NL3-2C	1.01	mesokurtic
NL3-2D	0.99	mesokurtic
NL3-8A	0.96	mesokurtic
NL3-8B	1.06	mesokurtic
NL3-8C	1.21	leptokurtic
NL3-8D	0.88	platykurtic
NL3-8E	1.11	leptokurtic

In the Wang, the average means is medium silt. The average degree of sorting (So) is very poorly sorted. Average skewness (Sk) has very positive skewed. Average kurtosis has mesokurtic. This means the value close to a normal distribution.

Table 5.10 Sediment characteristics of floodplain unit.

		Lower floodplain	Upper floodplain
mean	min	0.50 (c sand)	-1.38 (v f pebble)
	max	9.60 (clay)	5.17 (m silt)
	av.	5.44 (m silt)	1.67 (m sand)
sorting	min	1.25 (p sorted)	1.26 (p sorted)
	max	6.09 (e p sorted)	4.45 (e p sorted)
	av.	3.75 (v p sorted)	2.33 (v p sorted)
skewness	min	-0.03 (symmetrical)	-0.04 (symmetrical)
	max	0.58 (v p skewed)	0.68 (v p skewed)
	av.	0.26 (p skewed)	0.26 (p skewed)
kurtosis	min	0.84 (platykurtic)	0.92 (mesokurtic)
	max	1.75 (v leptokurtic)	3.2 (e leptokurtic)
	av.	1.08 (mesokurtic)	1.55 (v leptokurtic)

Table 5.11 Sediment characteristics of natural levee unit.

		The Ping	The Wang
mean	min	1.17 (m sand)	6.40 (m silt)
	max	5.7 (c silt)	7.65 (f silt)
	av.	4.04 (v c silt)	6.98 (m silt)
sorting	min	0.72 (m sorted)	2.62 (v p sorted)
	max	3.08 (v p sorted)	3.72 (v p sorted)
	av.	2.16 (v p sorted)	3.34 (v p sorted)
skewness	min	0 (symmetrical)	0.02 (symmetrical)
	max	0.62 (v p skewed)	0.72 (v p skewed)
	av.	0.39 (v p skewed)	0.39 (v p skewed)
kurtosis	min	0.99 (mesokurtic)	0.96 (mesokurtic)
	max	2.38 (v leptokurtic)	1.15 (leptokurtic)
	av.	1.51 (v leptokurtic)	1 (mesokurtic)

Point bar and sand bar units

2 samples were collected from point bar and 5 samples were collected from sand bar. All of samples were collected by surface sampling. Figure 5.35 shows histograms of size distribution from point bar and sand bar units. Sample PB4-1 is composed of coarse to very coarse sand up to 35 %. Sample no. PB5-5 is composed of pebbles up to 42 % with very coarse sand up to 37 %. Histogram of size distribution from sample no. SB5-2 contains large amount of pebble size. Sample no. SB5-7 shows maximum percent in medium sand size. Samples no. SB5-1 and SB5-3 show maximum percent of very coarse sand up to 50 %. Sample no. SB5-6 shows maximum percent in very fine pebble size.

In Figure 5.36-above, the curves represent the frequency of grain size samples from point bar and sand bar units. From these curves, most of samples show uni-modal character. The statistic values of the sediments from cumulative frequency curves (Figure 5.36-below) are presented in Tables 5.12-5.15.

The summary of sediment characteristics of point bar and sand bar units are shown in Table 5.16. In point bar unit, the average means is very coarse sand. The average degree of sorting (So) is moderately sorted. Average skewness (Sk) has symmetrical. Average kurtosis has mesokurtic. This means the value close to a normal distribution.

In sand bar unit, the average means is very coarse sand. The average degree of sorting (So) is poorly sorted. Average skewness (Sk) has symmetrical. Average kurtosis has mesokurtic. This means the value close to a normal distribution.

Figure 5.37 shows relationship of phi sorting and phi mean of samples from floodplain unit (a), natural levee unit (b), and point bar unit and sand bar unit (c). Only sand size sediments can be compared equivalently with fluvial sand of Briggs (1977). Figure 5.38 shows relationship of kurtosis and skewness of samples from floodplain unit (a), natural levee unit (b), and point bar unit and sand bar unit (c).

Relationship of phi sorting and phi mean of all samples from the study area is shown in Figure 5.39. Figure 5.40 shows relationship of kurtosis and skewness of all samples from the study area.

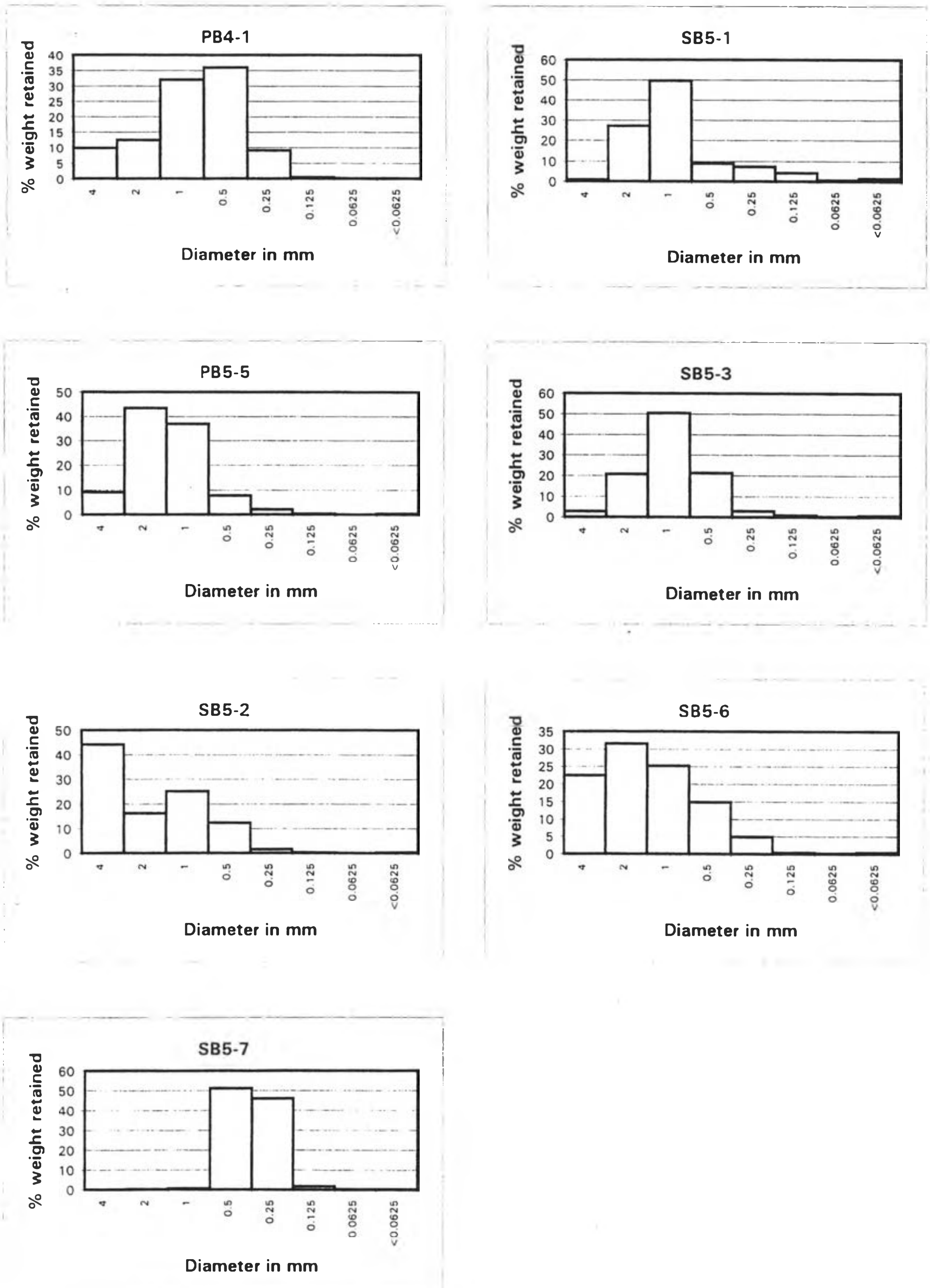

Figure 5.35 Histogram of size distribution from point bar and sand bar unit show pebbly to coarse sand.

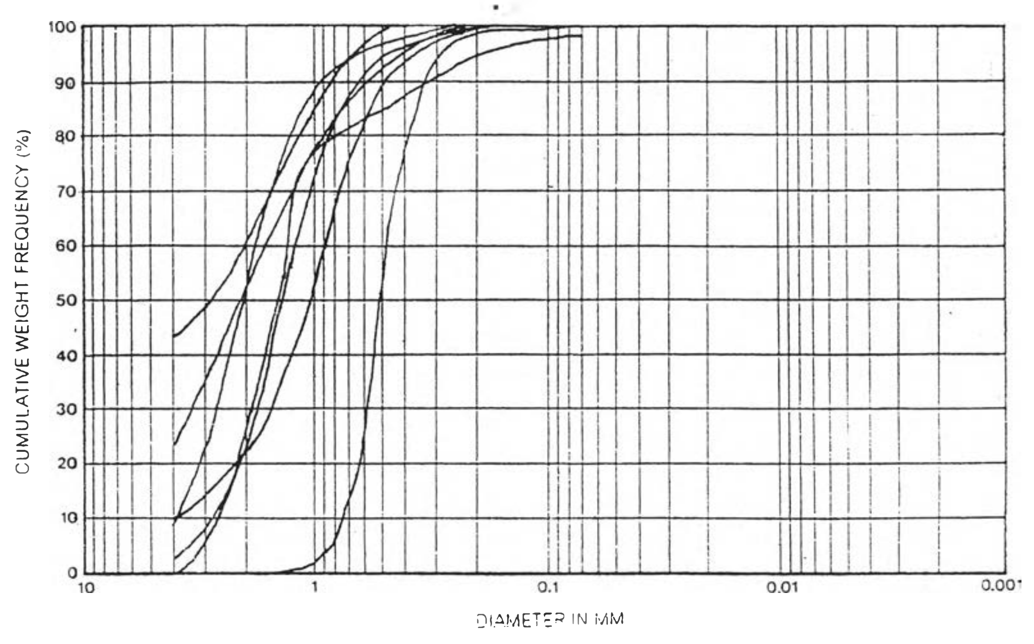

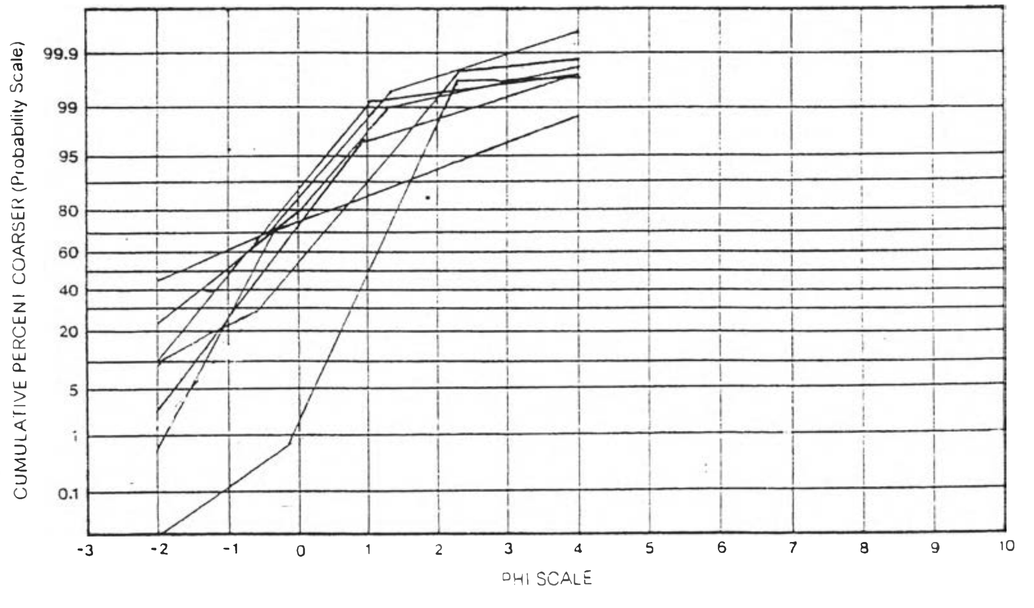

Figure 5.36 Two types of compilation plots of samples from point bar and sand bar unit. S-curve when using arithmetic ordinate scale cumulative against log-scale of diameters (above) and most of curves when plot by using probability cumulative against diameters in phi scale (below).

Table 5.12 Size distribution of samples from point bar and sand bar unit compare with standard phi mean from Friedman and Sander, 1978.

Sample	Values of mean	Size
PB4-1	-0.18	very coarse sand
SB5-7	1.00	coarse sand
PB5-5	-0.97	very coarse sand
SB5-3	-0.48	very coarse sand
SB5-2	-1.79	very fine pebbles
SB5-6	-1.08	very fine pebbles
SB5-1	-0.37	very coarse sand

Table 5.13 Comparison of sand samples from point bar and sand bar unit based on sorting values, compare with standard sorting term of Briggs (1977).

Sample	Values of sorting	Sorting class
PB4-1	0.94	moderately sorted
SB5-7	0.47	moderately well sorted
PB5-5	0.84	moderately sorted
SB5-3	0.75	moderately sorted
SB5-2	2.07	very poorly sorted
SB5-6	1.25	poorly sorted
SB5-1	0.89	moderately sorted

Table 5.14 Classification of samples from point bar and sand bar unit into skewness values described based on standard term by Briggs (1977).

Sample	Values of skewness	Skewness class
PB4-1	-0.12	negatively skewed
SB5-7	0.00	symmetrical
PB5-5	-0.02	symmetrical
SB5-3	0.03	symmetrical
SB5-2	-0.44	very negatively skewed
SB5-6	-0.06	symmetrical
SB5-1	0.51	very positive skewed

Table 5.15 Classification of samples from point bar and sand bar unit into kurtosis description term based on phi scale and compared with standard class of Briggs (1977).

Sample	**Values of kurtosis**	**Kurtosis class**
PB4-1	1.10	mesokurtic
SB5-7	1.05	mesokurtic
PB5-5	0.92	mesokurtic
SB5-3	0.98	mesokurtic
SB5-2	0.89	platykurtic
SB5-6	0.98	mesokurtic
SB5-1	1.45	leptokurtic

Table 5.16 Sediment characteristics of point bar and sand bar unit.

		Point bar	Sand bar
mean	min	-0.97 (v c sand)	-1.08 (v f pebble)
	max	-0.18 (v c sand)	1 (c sand)
	av.	-0.58 (v c sand)	-0.55 (v c sand)
sorting	min	0.84 (m sorted)	0.47 (m w sorted)
	max	0.94 (m sorted)	2.07 (v p sorted)
	av.	0.89 (m sorted)	1.09 (p sorted)
skewness	min	-0.12 (n skewed)	-0.44 (v n skewed)
	max	-0.02 (symmetrical)	0.51 (v p skewed)
	av.	-0.07 (symmetrical)	0.01 (symmetrical)
kurtosis	min	0.92 (mesokurtic)	0.89 (platykurtic)
	max	1.10 (mesokurtic)	1.45 (leptokurtic)
	av.	1.01 (mesokurtic)	1.07 (mesokurtic)

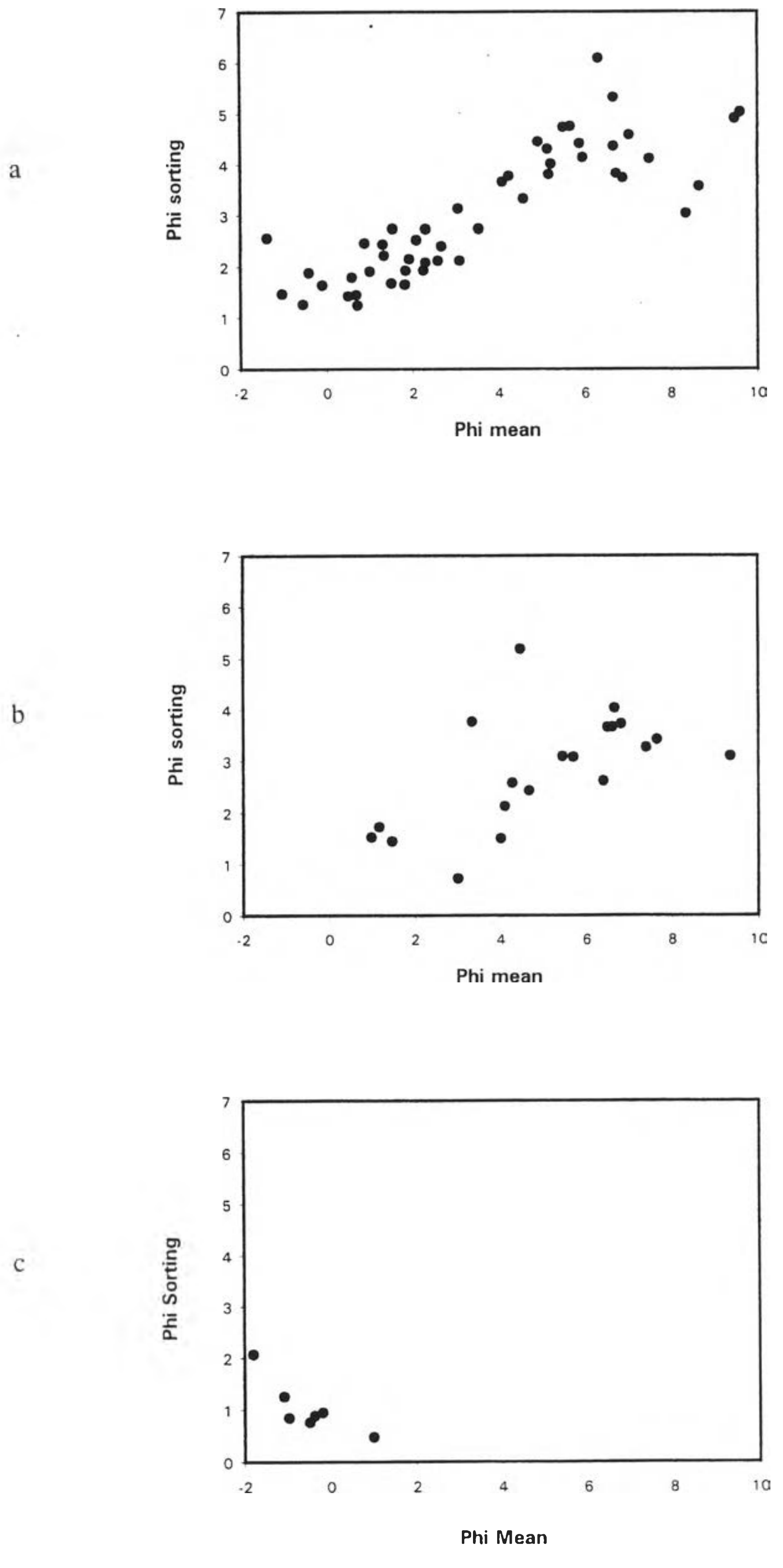

Figure 5.37 Relationship of phi sorting and phi mean of samples from floodplain unit (a), natural levee unit (b) and point bar and sand bar unit (c).

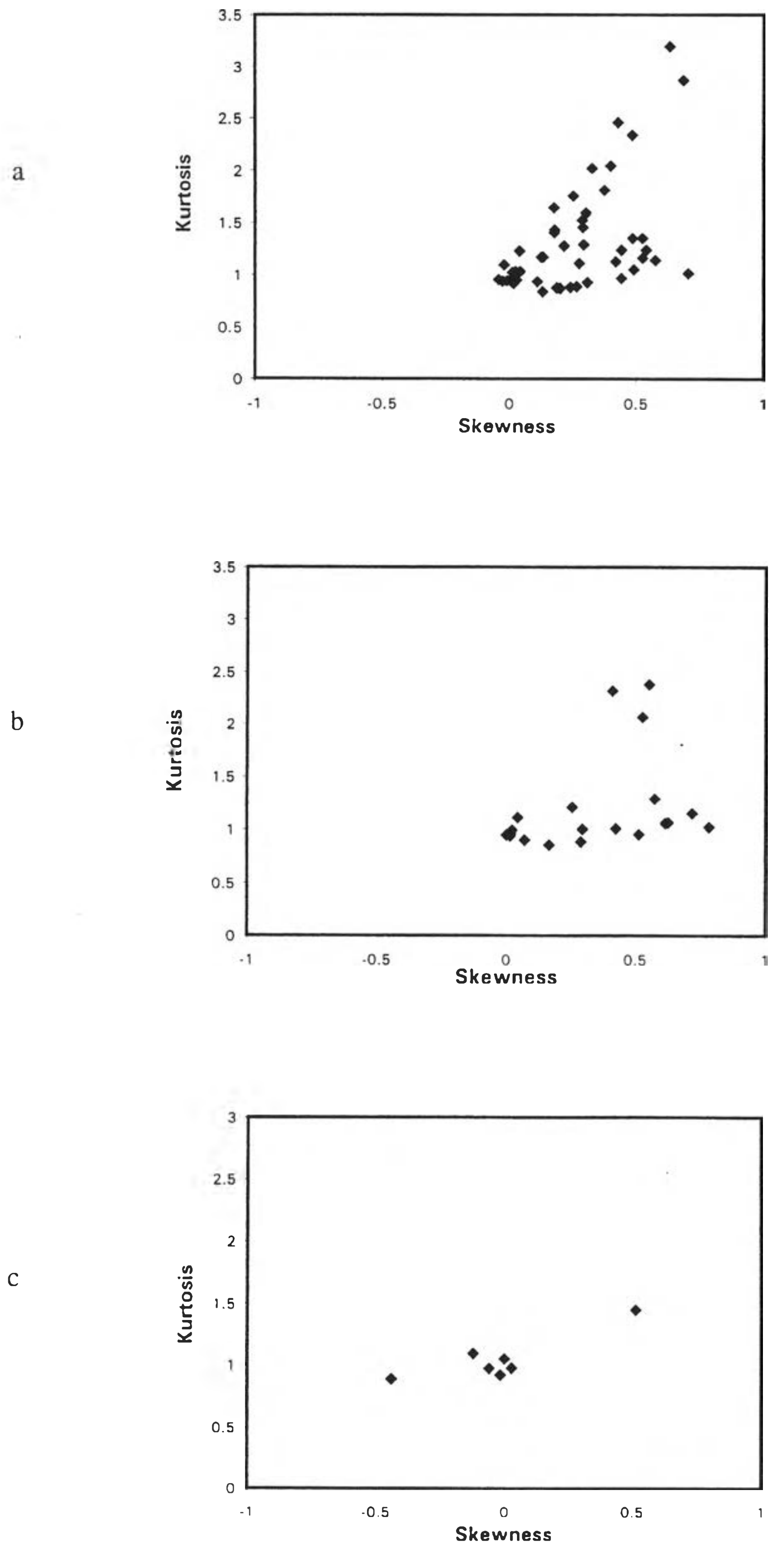

Figure 5.38 Relationship of kurtosis and skewness of samples from floodplain unit (a), natural levee unit (b) and point bar and sand bar unit (c).

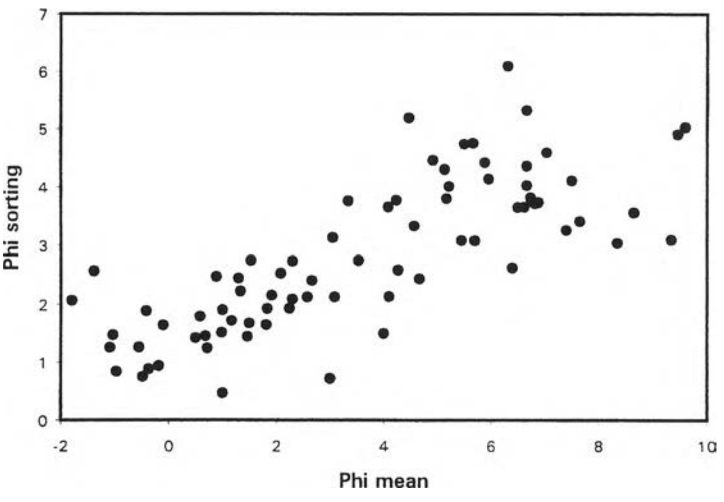

Figure 5.39 Relationship of phi sorting and phi mean of samples from the study area.

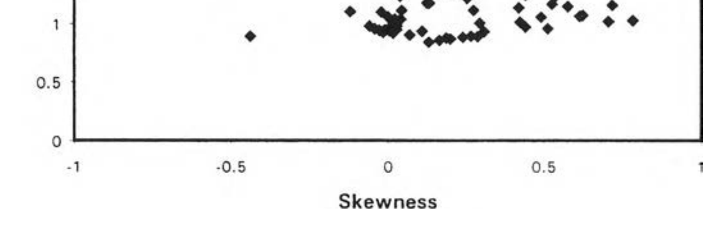

Figure 5.40 Relationship of kurtosis and skewness of samples from the study area.

From the results of particle size analysis, the fluvial deposits in the study area can be grouped in to 3 major environments of deposition:

1. Flood basin deposits: They are fine-grained sediment deposits formed during heavy floods when river water flows over the levees into the flood basin. They are floodplain unit in the study area.
2. Bank deposits: They are sediment deposits formed on the riverbanks and are produced during flood periods. In the study area, they are natural levee unit.
3. Channel deposits: They are sediment deposits formed mainly of the activity of river channels. They are point bar unit and sand bar unit in the study area.